Bull. Pharm. Sci., Assiut University, Vol. 45, Issue 1, 2022, pp. 201-222.

Bulletin of Pharmaceutical Sciences
Assiut University
Website: http://bpsa.journals.ekb.eg/
e-mail: bullpharm@aun.edu.eg

SYNTHESIS, MOLECULAR MODELING STUDY, AND BIOLOGICAL EVALUATION OF N-ACYL-ANTHRANOYLANTHRANILIC ACID DERIVATIVES AND THEIR CYCLIZED BENZOXAZINONES AS NOVEL HIV-1 NONNUCLEOSIDE REVERSE TRANSCRIPTASE INHIBITORS

Hossam. M. Abdel-Aziz[1,2], Ahmed M. Ali[1], Atef A-M. Abdel-Hafez[1] and Adel F. Youssef *[1]

[1]*Department of Medicinal Chemistry, Faculty of Pharmacy, Assiut University, Assiut, 71526, Egypt.*
[2]*Present Affiliation, Department of Medicinal Chemistry, Faculty of Pharmacy, South Valley University, Qena, 83511, Egypt.*

*N-Acylanthranoylanthranilic acids (**5a–n**) and their cyclized 4H-benzo [d][1,3] oxazin-4-one derivatives (**6a–n**) were prepared via a three-step process. The synthesized compounds were then screened to determine their human immunodeficiency virus (HIV-1) nonnucleoside reverse transcriptase (NNRT) inhibition activity. The half-maximal inhibitory concentrations of the compounds, (IC_{50}), were found to be in the range of 30 nM–123 µM, using nevirapine as a reference HIV drug. The reverse transcriptase inhibition activity of the compounds was shown to be distinctly affected by the cyclized motif and the nature of the appended N-acyl moiety. Selected active compounds, **5a**, **6d**, **6h**, and **6k** (IC_{50} <1 µM), exhibit high selectivity index SI= CC_{50} / IC_{50} . Most of the designed compounds fulfill Lipinski's requirements of druggability. Molecular docking studies reveal H–π, H–O (N), π–π, and halogen bonding between the docked compounds and the residues within the allosteric binding pocket close to the RT active site. The highest occupied molecular orbital (HOMO) and the lowest unoccupied molecular orbital (LUMO)- derived energy descriptors are shown to be useful predictive tools for reverse transcriptase inhibition (RTI) activity and in silico binding to mutant nucleophilic side chain residues in the nonnucleoside inhibitor binding pocket motif.*

Keywords: *NNRTIs; Anthranilamide; Benzoxazinnone; Docking; SAR*

INTRODUCTION

By 2019, the global number of people with HIV had reached approximately 38 million, of which 95.3% and 4.7% were adults and children, respectively.[1] Despite the efficacy of antiretroviral therapy in halting the transmission of the virus and progression of the disease, there is still no cure for HIV, which means that it remains a global public health issue.[2] Besides the little economic growth of nations impacted by AIDS, it has been predicted that the COVID-19 pandemic could worsen this situation.[3]

A meticulous study on why and where an HIV cure is needed, and how it might be achieved, was undertaken by Deeks *et al*.[4] Antiretroviral medicines used in combination therapy for the treatment of HIV infection can be classified into five categories: entry inhibitors (fusion and attachment), nucleoside reverse transcriptase inhibitors (NRTIs), nonnucleoside reverse transcriptase inhibitors (NNRTIs), protease inhibitors (PIs) and integrase strand transfer inhibitors (ISTIs).[5] However, when it comes to the management of AIDS, this issue is still complex because of the high tendency toward the development of drug

Received in 28/12/2021 & Accepted in 11/3/2022

*Corresponding author: Adel F. Youssef, E-mail: adelfawzy@ aun.edu.eg

resistance, chronic drug toxicity, poor tolerability toward drugs, therapy adjustment after treatment failure, and unwanted side effects of treatment. With this in mind, one global healthcare target is the multidisciplinary search for new inhibitors that exhibit lower chronic toxicity and possibly active mechanisms and patterns that are effective against mutant strains compared with the approved drugs that are currently on the market.[6]

The unique antiviral potency and mechanism of action of NNRTIs allow them to be effectively used in highly active and different combination therapy regimens used in the treatment of HIV-1. However, the low genetic barrier of the first generation of NNRTIs, shown in Figure 1, resulted in the rapid emergence of the most common drug-resistant mutant forms of HIV, Lys103Asn, and Tyr181Cys, which led to drug resistance toward the HIV drugs nevirapine and efavirenz.[7] In another study, the HIV mutant Pro236Leu was shown to develop resistance toward delavirdine.[8] Although the second-generation HIV drug etravirine and its α,β-diaminopyrimidine analog rilpivirine have been shown to inhibit single mutants that have evolved as a result of first-generation therapy, they fail to suppress the most resistant single Glu138Lys and double (Lys103Asn/ Tyr181Cys) mutants, together with exhibiting side effects.[7]

These results have motivated the search for new NNRTIs with different chemical structures and improved therapeutic profiles. Functionalized analog-based NNRTIs have been reviewed by Shirvani *et al*.,[9] which show different patterns of reverse transcriptase inhibition (RTI) activity, toxicity, and drug resistance. The reported molecular analog approaches have dealt with motifs featuring a central heteroaryl or aryl nucleus such as pyrimidine, pyridine, indole, isatin, thiadiazine, benzothiadiazine, dihydroquinoxalinone, benzoxazinone, and benzene,[10] functionalized with substituted phenyl, benzyl, naphthyl, and alkyl moieties,[11] where the linked moieties were arranged to accommodate interactions with residues in the HIV-1 RT allosteric nonnucleoside inhibitor binding pocket (NNIBP). An RTI was designed on the basis of structural bioisosterism[12] *via* the replacement of low-efficiency thiophene [3,2-*d*] pyrimidine derivatives with thiophene [2,3-*d*] pyrimidine analogs, which were found to enhance anti-HIV-1 activity compared with etravirine against all of the tested NNRTI-resistant HIV-1 strains and showed improved solubility and optimal pharmacokinetic properties.

In summary, the research results in two critical requirements that lead to the design of improved HIV-1 NNRTI molecules. The first request is the ligand's ability to bind the target nonpolar and polar residues in the nonnucleoside inhibitor binding pocket (NNIBP). The second request is the controlled conformational flexibility of the ligand to optimize the productive fitting in the flexible NNIBP and in the modified mutant pocket.

In this work, the design and the synthesis of two new subclasses of *ortho*-substituted aniline scaffold were achieved, the structures of which are shown in Figure 2. In the first series, the intermediate building block features the 2-(2-aminobenzamido)benzoic acid, whereas the second series building block features the 2-aminophenyl-*4H*-benzo[*d*]-1,3-oxazin-4-one. Both motifs were coupled with the *N*-acyl moieties to yield the final products (5a–n) and (6a–n), which mimic the "butterfly-like" conformation of many active NNRTIs.[9–12] Docking of the prepared compounds into the RT allosteric site, shown in Table S1, revealed their stabilized conformations achieved *via* hydrogen bonding, π–π stacking, and halogen bonding interactions. The RTI activity of all of the target compounds (5a–n) and (6a–n) was evaluated to determine their half-maximal inhibitory concentration (IC_{50}) values, with the most active and suitable drug candidates selected and their 50 % cytotoxic concentration (CC_{50}), determined against HeLa cells. The relationship between the RTI activity and molecular structure was also investigated.

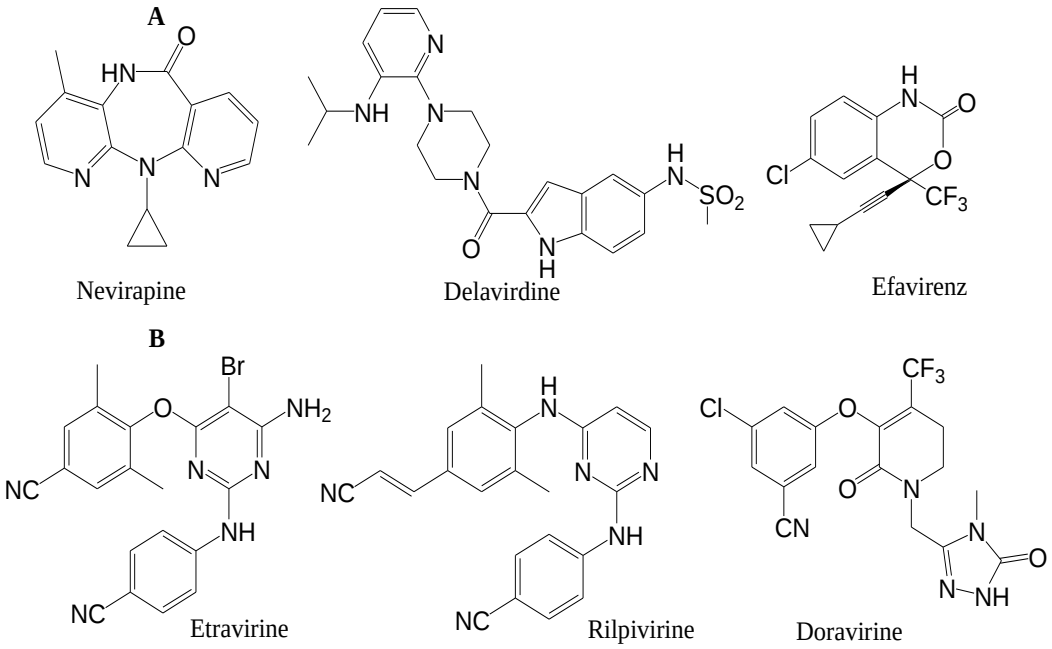

Fig. 1: NNRTIs approved by USA FDA. A) first generation, and B) second generation

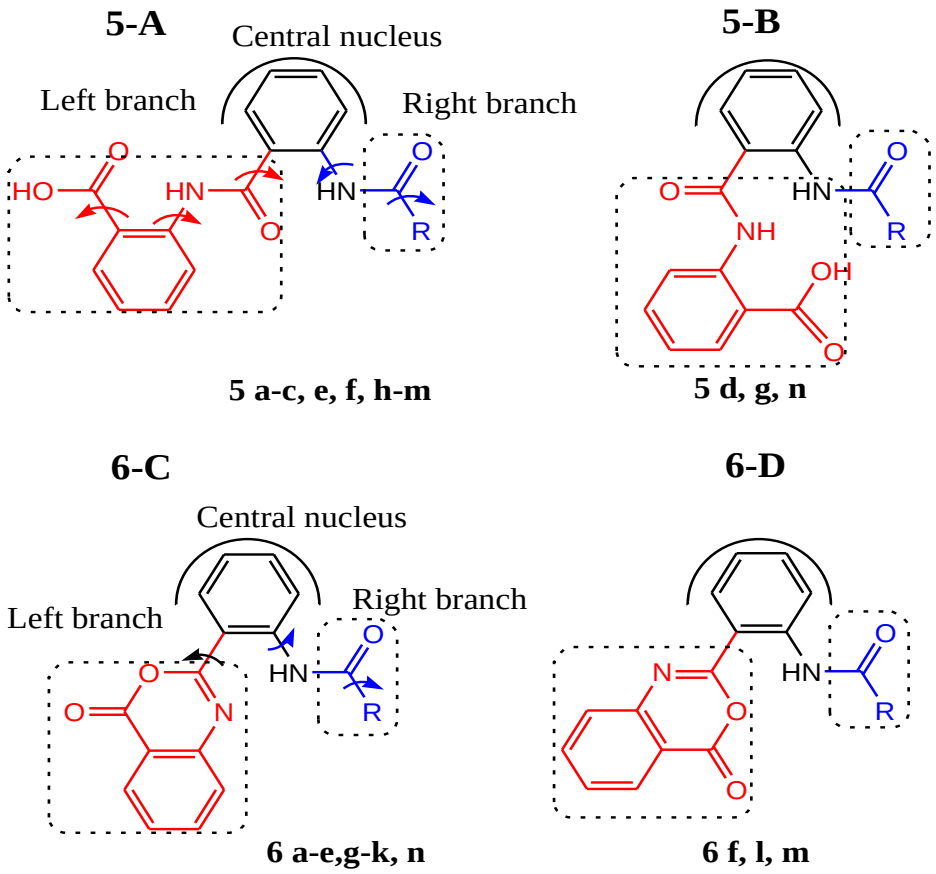

Fig. 2: General structures of the targeted N- acyl-*o*- substituted aniline derivatives **5a-n** and **6a-n**. The left branch (red) was kept unchanged within each series while the right branch N-acyl moiety (blue) carried the variable R= a-n groups listed in Scheme 1. The "butterfly- like" conformations of **5-A**, **5-B** and **6-C**, **6-D** are the bound- state of the least energy conformer poses of the molecules docked in the NNIBP.

MATERIALS AND METHODS

Materials

General Notes

All the chemicals were commercially available reagent grades and were used without further purification. Melting points in degrees Celsius (°C) were determined on Stuart melting point apparatus (Stuart Scientific, England) and were uncorrected. NMR data were performed on Bruker Spectrophotometer (400 MHz for ^{1}H-NMR and 100 MHz for ^{13}C-NMR), Faculty of Science, Suhag University, Suhag, Egypt. Chemical shifts are expressed in δ values (ppm) relative to tetramethylsilane (TMS) as an internal standard. Coupling constants (J) for ^{1}H-NMR were given in Hz and expressed as: (s) for singlet, (d) for doublet, (t) for triplet, (q) for the quartet, and (m) for multiplet. DMSO-d_6 was used as solvent. IR data were performed on FT-IR using KBr disc at Faculty of Pharmacy, Assiut University, Assiut, Egypt. Elemental analyses were performed in the Regional Center for Mycology and Biotechnology, Al-Azhar University, Nasr City, Cairo, Egypt. X-Ray crystallography was performed on Bruker D8 Venture TXS diffractometer, X-Ray Laboratory, Department of Chemistry, University of Munich, Butenandt str. 5-13, D-81377 Munich, Germany. The molecular modeling studies were carried out at the Department of Medicinal Chemistry, Faculty of Pharmacy, Assiut University, Assiut, Egypt using Molecular Operating Environment (MOE 2019.0101, Chemical Computing Group, Canada) as the computational software.

The HIV-1 RTI assay was carried out in VACSERA (Holding Company For Biological Products & Vaccines SAE, Agouza, Giza, Egypt). The HIV-1 RTI (IC_{50}) was determined in the presence of various concentrations of the tested compounds using a Roche colorimetric HIV-1 RT assay kit following the protocol provided by the manufacturer.

Cytotoxicity evaluation assay was performed in the Regional Center for Mycology and Biotechnology, Al-Azhar University, Nasr City, Cairo, Egypt.

Chemistry

Synthesis of 2-(2-aminobenzamido) benzoic acid 3[13]

Yield 1.5 g (58%); m.p (196-198°C), reported m.p (201-202°C)

Preparation of the acid chlorides 4a-m according to the described convential method [14]

a: Benzoyl chloride, b: 4-chlorobenzoyl chloride, c: 4-methylbenzoyl chloride, d: 2-(4-methoxyphenyl) acetyl chloride, e: 3-phenylpropanoyl chloride , f: 2-(naphthalene-1-yl)acetyl chloride, g: 2-(2,4-dichlorophenyl) acetyl chloride, h: hexanoyl chloride, i: nicotinoyl chloride, j: pentanoyl chloride, k: 3,4,5- trimethoxybenzoyl chloride, l: 2-[1- (4-chlorobenzoyl)- 5-methoxy-2-methylindol- 3-yl] acetyl chloride, m: chloroacetyl chloride. The obtained acid chlorides were used directly in the following reactions without further purification.

General method adopted for the synthesis of 2- (2-acylaminobenzamido) benzoic acids 5a-m [15]

To the stirred solution of 3 (0.512 g, 0.002mol) in dioxane (30 ml), an equimolar ratio of the appropriate acid chloride 4a-m was added dropwise at room temperature. Stirring was continued overnight at room temperature. After completion of the reaction, monitored by TLC (using a mixture of ethylacetate-hexane (4:1), water was added and the precipitate was filtered off and dried at 45 °C, and recrystallized from the specified solvent.

2-(2-Benzamidobenzamido) benzoic acid 5a

White crystals (n-butanol-ethanol 95% 4:1); yield (0.63 g, 90%); m.p. (found 220-222°C, not reported), FT-IR: 3129 (sp^2C-H); 2500-3500 (broad band COOH);1695 (carboxylic C=O);1661 (amidic C=O);1217 (C-O); 751 (*o*-disubstituted benzene).^{1}H NMR and ^{13}CNMR are in agreement with those pulished previously[13]. Anal. Calcd. for $C_{21}H_{16}N_2O_4$: C, 69.99; H, 4.48; N, 7.77. Found: C, 70.13; H, 4.56; N, 7.94.

2-(2-(4-Chlorobenzamido)benzamido) benzoic acid 5b

White crystals (n-butanol-ethanol 95% 4:1); yield (0.53 g, 69%) m.p. (239.5-240.5°C);

FT-IR: 3150(sp^2C-H); 2500-3500 (broad band COOH); 1686 (carboxylic C=O); 1660 (amidic C=O);1221(C-O);748(*o*-disubstituted benzene); 843(*p*-disubstituted benzene); ^{1}H NMR**;** 12.02 (s, 1H,NH), 11.61 (s, 1H,NH), 8.55 (d, *J* = 7.7 Hz, 1H), 8.35 (d, *J*= 8.2 Hz, 1H), 8.03 (dd, *J* = 7.9, 1.5 Hz, 1H), 7.98 – 7.89 (m, 3H), 7.71 – 7.54 (m, 4H), 7.35 (t, *J* = 7.5 Hz, 1H), 7.28 – 7.21 (m, 1H); ^{13}C NMR**;** 170.10 (carboxylic C=O) , 167.2 (amidic C=O) and 164.3 (amidic C=O) , 140.7 , 138.7 , 137.3 , 134.5 , 133.6 , 133.0 , 131.6 , 129.5 , 129.3 , 128.5 , 124.6 , 124.5 , 123.9 , 122.8, 121.2 and 118.1; Anal. Calcd. for $C_{21}H_{15}ClN_2O_4$: C, 63.89; H, 3.83; N, 7.10. Found: C, 63.97; H, 4.06; N, 7.36.

2-(2-(4-Methylbenzamido)benzamido) benzoic acid 5c

White crystals (n-butanol-ethanol 95% 4:1); yield (0.51g,70%); m.p. (235.5-237.5^{o}C)**;** FT-IR: 2948 (sp^3C-H); 2500-3500 (broad band COOH); 1682 (carboxylic C=O); 1660 (amidic C=O); 1238 (C-O); 750 (*o*-disubstituted benzene); 839 (*p*-dsubstituted benzene); ^{1}H NMR**;** 12.05 (s, 1H, NH), 11.65 (s, 1H, NH), 8.55 (d, *J* = 8.3 Hz, 1H), 8.46 (d, *J* = 8.3 Hz, 1H), 8.04 (d, *J* = 7.7 Hz, 1H), 7.92 (d, *J* = 7.7 Hz, 1H), 7.83 (d, *J* = 7.8 Hz, 2H), 7.67-7.31 (m, , 6H), 2.38 (s, 3H); ^{13}C NMR**;** 170.1 (carboxylic C=O), 167.4 (amidic C=O) and 165.1 (amidic C=O), 142.6, 140.7 , 139.3 , 134.5 , 133.1 , 132.1 , 131.6 , 129.8 , 128.4 , 127.6 , 124.2 , 124.04 , 123.50 , 122.3 , 121.3 and 118.2 , 21.4 ; Anal. Calcd. for $C_{22}H_{18}N_2O_4$: C,70.58; H, 4.85; N, 7.48. Found**:** C,70.84; H, 4.69; N, 7.32. (in the original source **[13]** the compound purchased from ChemBridge Corp., analyzed with LCMS, and used without further NMR characterization).

2-(2-(2-(4-Methoxyphenyl)acetamido) benzamido) benzoic acid 5d

White crystals (n-butanol-ethanol 95% 4:1); yield (0.62g, 79.4%); m.p. (214.5-215.5^{o}C)**;** FT-IR: 3650 (NH); 3118 (sp^2C-H); 2929, 2830 (sp^3C-H); 2500-3500 (broad band COOH); 1682 (carboxylic C=O);1660 (amidic C=O); 1244 (C-O); 756 (*o*-disubstituted benzene); 827 (*p*-disubstituted benzene);^{1}H NMR**;** 11.85 (s, 1H, NH), 10.57 (s, 1H, NH), 8.53 (dd, *J* = 8.4, 0.7 Hz, 1H), 8.12 (d, *J* = 7.7 Hz, 1H), 8.04 (dd, *J* = 7.9, 1.6 Hz, 1H), 7.76 (dd, *J* = 7.9, 1.4 Hz, 1H), 7.68 (ddd, *J* = 9.8, 7.0, 2.6 Hz, 1H), 7.59 – 7.51 (m, 1H), 7.30 – 7.18 (m, 4H), 6.87 – 6.81 (m, 2H), 3.72 (s, 3H, CH_3), 3.61 (s, 2H, CH_2); ^{13}C NMR**;** 170.19 (carboxylic C=O) , 170.1 (amidic C=O) and 166.6 (amidic C=O) , 158.6 , 140.9 , 138.1 , 134.5 , 132.5 , 131.6 , 130.8 , 128.2 , 127.4 , 125.1, 124.2, 123.7 , 122.6 , 120.88 , 117.63 and 114.2 , 55.4 (OCH_3) , 43.3 (CH_2); Anal. Calcd. for $C_{23}H_{20}N_2O_5$: C, 68.31; H, 4.98; N, 6.93. Found: C, 68.54; H, 5.04; N, 7.21.

2-(2-(3-Phenylpropanamido)benzamido) benzoic acid 5e

White crystals (n-butanol-ethanol 95% 4:1); yield (0.6 g, 79%); m.p. (200-201^{o}C)**;** FT-IR: 3137 (sp^2C-H); 2920 (sp^3C-H); 2500-3500 (broad band COOH); 1688 (carboxylic C=O);1668 (amidic C=O);1230 (C-O);^{1}H NMR**;** 11.87 (s, 1H, NH), 10.51 (s, 1H, NH), 8.65 – 8.59 (m, 1H), 8.10 – 8.02 (m, 2H), 7.78 (dd, *J* = 7.8, 1.3 Hz, 1H), 7.72 – 7.64 (m, 1H), 7.60 – 7.52 (m, 1H), 7.30 – 7.12 (m, 7H), 2.88 (t, *J* = 7.7 Hz, 2H), 2.64 (t, *J* = 7.7 Hz, 2H); ^{13}C NMR **;** 170.8 (carboxylic C=O) , 170.1 (amidic C=O) and 166.7 (amidic C=O) , 141.3 , 141.2 , 137.8 , 134.5 , 132.4 , 131.6 , 128.7 , 128.6 , 128.4 , 126.40 , 125.53 , 124.3 , 123.7 , 122.9 , 120.9 , 117.6, 38.7 and 31.1 ; Anal. Calcd. for $C_{23}H_{20}N_2O_4$: C, 71.12; H, 5.19; N,7.21. Found: C,71.3; H, 5.34; N, 7.38**.**

2-(2-(2-(Naphthalen-1-yl) acetamido) benzamido) benzoic acid 5f

White crystals (n-butanol-ethanol 95% 4:1); yield (0.6 g, 73%); m.p. (210.5-211.5^{o}C); FT-IR: 3150 (sp^2C-H); 2850 (sp^3C-H); 2500-3500 (broad band COOH); 1690 (carboxylic C=O);16650 (amidic C=O);1220 (C-O); ^{1}H NMR**;** 11.83 (s, 1H, NH), 10.67 (s, 1H, NH), 8.40 (d, *J* = 8.3 Hz, 1H), 8.15 (d, *J* = 8.3 Hz, 1H), 8.03 (dt, *J* = 6.5, 2.4 Hz, 2H), 7.94 – 7.85 (m, 2H), 7.77 – 7.66 (m, 2H), 7.57 – 7.45 (m, 5H), 7.24 (dd, *J* = 10.9, 4.4 Hz, 2H), 4.20 (s, 2H); ^{13}C NMR**;** 170.1 (carboxylic C=O) , 169.8 (amidic C=O) and 166.57 (amidic C=O) , 140.8 , 138.1 , 134.5 , 133.9 , 132.5 , 132.4 , 131.90, 131.5 , 128.90 , 128.1 , 128.0, 126.6 , 126.1, 126.0 , 124.8 , 124.4 , 124.2 , 123.7 , 122.5 , 120.9 and 117.6 , 41.8 ; Anal. Calcd. for $C_{26}H_{20}N_2O_4$: C,73.57; H, 4.75; N,6.6. Found: C,73.69; H, 4.81; N, 6.87.

2-(2-(2-(2,4-Dichlorophenyl)acetamido) benzamido)benzoic acid 5g

White crystals (n-butanol-ethanol 95% 4:1); yield (0.55 g, 68%); m.p. (260.5-261.5°C); FT-IR: 3673, 3646 (amidic NH); 2986 (sp^3C-H); 2500-3500 (broad band COOH);1693 (carboxylic C=O); 1651 (amidic C=O);1217 (C-O); 753 (*o*-disubstituted benzene; ^{1}H NMR**;** 11.94 (s, 1H, NH), 10.67 (s, 1H, NH), 8.50 (d, *J* = 7.9 Hz, 1H), 8.18 (t, *J* = 9.0 Hz, 1H), 8.08 – 8.01 (m, 1H), 7.82 – 7.74 (m, 1H), 7.72 – 7.52 (m, 3H), 7.50 (d, *J* = 8.3 Hz, 1H), 7.45 – 7.39 (m, 1H), 7.32 – 7.21 (m, 2H), 3.86 (s, 2H) ; ^{13}C NMR**;** 170.1 (carboxylic C=O) , 168.2 (amidic C=O) and 166.7 (amidic C=O) , 140.9 , 138.0 , 135.3 , 134.6 , 134.1 , 133.1 , 132.7 , 132.6 , 131.6 , 129.1 , 128.1 , 127.9 , 124.7 , 124.4 , 123.8, 122.5 , 120.8, 117.6, and 41.3; Anal. Calcd. for $C_{22}H_{16}Cl_2N_2O_4$: C, 59.61; H, 3.64; N, 6.32. Found: C, 59.87; H, 3.8; N, 6.59.

2-(2-(Hexanamido)benzamido)benzoic acid 5h

White crystals (ethanol 95% - water 4:1) ; yield (0.425g,60.8%); m.p. (191-192°C); FT-IR: 2952-2868 (sp^3C-H); 2500-3500 (broad band COOH); 1681 (carboxylic C=O); 1654 (amidic C=O); 1235(C-O); ^{1}H NMR**;** 11.85 (s, 1H,NH), 10.49 (s, 1H,NH), 8.60 (d, *J*= 8.2 Hz, 1H), 8.09 – 8.01 (m, 2H), 7.78 (dd, *J*= 7.8, 1.0 Hz, 1H), 7.70 – 7.63 (m, 1H), 7.60 – 7.52 (m, 1H), 7.31 – 7.19 (m, 2H), 2.29 (t, *J*= 7.4 Hz, 2H), 1.54 (m, 2H), 1.23 (dd, *J* = 8.7, 5.2 Hz, 4H), 0.81 (t, *J* = 6.6 Hz, 3H); ^{13}C NMR**;**171.71 (carboxylic C=O) , 170.1 (amidic C=O) and 166.8 (amidic C=O) , 141.1 , 137.9 , 134.5 , 132.4 , 131.6 , 128.4 , 125.6 , 124.2 , 123.6 , 122.9 , 120.9, 117.6 , 37.1, 31.2 , 25.1, 22.3 , 14.2; Anal. Calcd. for $C_{20}H_{22}N_2O_4$: C, 67.78; H, 6.26; N, 7.9. Found: C, 68.06; H, 6.4; N, 8.13.

2-(2-(Nicotinamido) benzamido)benzoic acid 5i[16]

White crystals (n-butanol-ethanol 95% 4:1); yield (0.52 g, 71.4%); m.p. (238-240°C); FT-IR: 3685 (amidic NH); 3175 (sp^2C-H); 2500-3500 (broad band COOH);1770 (carboxylic C=O); 1688 (amidic C=O); 1220 (C-O); ^{1}H NMR; 11.99 (s, 1H, NH), 11.62 (s, 1H, NH), 9.10 (s, 1H), 8.78 (d, *J* = 4.6 Hz, 1H), 8.58 (d, *J* = 8.4 Hz, 1H), 8.36 (d, *J* = 8.2 Hz, 1H), 8.30 – 8.23 (m, 1H), 8.04 (d, *J* = 7.9 Hz, 1H), 7.93 (d, *J* = 7.8 Hz, 1H), 7.67 (t, *J* = 7.8 Hz, 2H), 7.59 (dd, *J* = 7.6, 5.0 Hz, 1H), 7.37 (t, *J* = 7.6 Hz, 1H), 7.24 (t, *J* = 7.6 Hz, 1H); ^{13}C NMR**;** 170.0 (carboxylic C=O) , 167.2 (amidic C=O) and 163.9 (amidic C=O) , 152.7 , 148.5 , 140.5 , 138.5 , 135.4 , 134.5 , 132.9 , 131.6 , 130.6 , 128.4 , 124.8 , 124.2 , 123.9 , 123.0 , 121.3, 118.2 ; Anal. Calcd. for $C_{20}H_{15}N_3O_4$: C, 66.48; H, 4.18; N, 11.63. Found: C, 66.76; H, 4.25; N, 11.84

2-(2-(Pentanamido) benzamido)benzoic acid 5j

White crystals (ethanol 95%-water 4:1); yield (0.51 g, 75%); m.p. (195.5-197°C); FT-IR: 3062 (sp^2 C-H); 2952, 2869 (sp^3 C-H); 2500-3500 (broad band COOH);1675, 1656(amidic C=O);1228 (C-O); ^{1}H NMR**;** 13.57 (s, 1H, COOH), 11.81 (s, 1H, NH), 10.50 (s, 1H, NH), 8.59 (d, *J* = 8.3 Hz, 1H), 8.15 (d, *J* = 8.2 Hz, 1H), 8.05 (dd, *J* = 7.9, 1.1 Hz, 1H), 7.80 (d, *J* = 7.7 Hz, 1H), 7.72 – 7.62 (m, 1H), 7.56 (t, *J* = 7.8 Hz, 1H), 7.25 (dd, *J* = 17.1, 7.9 Hz, 2H), 2.33 (t, *J* = 7.4 Hz, 2H), 1.60 – 1.50 (m, 2H), 1.39 – 1.25 (m, 2H), 0.86 (t, *J* = 7.3 Hz, 3H); ^{13}C NMR**;** 171.6 (carboxylic C=O) , 170.0 (amidic C=O) and 167.0 (amidic C=O) , 141.0 , 138.1, 134.4 , 132.5 , 131.5 , 128.0 , 124.9 , 124.0 , 123.7 , 122.7, 121.1, 117.9, 37.0 , 27.5 22.1 , 14.0; Anal. Calcd. for $C_{19}H_{20}N_2O_4$: C, 67.05; H, 5.92; N, 8.23. Found: C, 67.26; H, 5.89, N, 8.37.

2-(2-(3, 4, 5-Trimethoxybenzamido) benzamido) benzoic acid 5k

White crtals (ethanol 95%); yield (0.711 g, 79%); m.p. (234.5-236 °C); FT-IR: 2944, 2839 (sp^3 C-H); 2500-3500 (broad band COOH);1658 (amidic C=O);1227 (C-O); ^{1}H NMR**;** 12.02 (s, 1H, NH), 11.54 (s, 1H, NH), 8.59 (d, *J* = 8.4 Hz, 1H), 8.38 (d, *J* = 8.3 Hz, 1H), 8.04 (d, *J* = 7.9 Hz, 1H), 7.91 (d, *J* = 7.8 Hz, 1H), 7.66 (t, *J* = 7.6 Hz, 2H), 7.34 (t, *J* = 7.6 Hz, 1H), 7.23 (d, *J* = 10.1 Hz, 3H), 3.86 (s, 6H, $2CH_3$), 3.76 (s, 3H); ^{13}C NMR**;** 170.0 (carboxylic C=O) , 167.2 (amidic C=O) and 164.9 (amidic C=O) , 153.3 , 141.3 , 140.8 , 139.1 , 134.4 , 132.9 , 131.6 , 130.3 , 128.3 , 124.3 , 123.9 , 122.5 , 121.1 , 118.0, 106.1, 60.7, 56.5; Anal. Calcd. for $C_{24}H_{22}N_2O_7$: C, 63.99; H, 4.92; N, 6.22. Found: C, 63.79; H, 4.81; N, 6.34.

2-(2-(2-(1-(4--Chlorobenzoyl)-5-methoxy-2-methylindol-3-yl) acetamido) benzamido)benzoic cid 5l

White crystals (ethanol 95%); yield (0.98 g, 82%); m.p. (219.5-221.5 ^{o}C); FT-IR: 3630 (NH); 2930, 2850 (sp^{3}C-H); 2500-3500 (broad band COOH); 1688 (carboxylic C=O);1661 (amidic C=O);1222 (C-O);^{1}H NMR**;** 13.64 (s, 1H, COOH), 11.83 (s, 1H, NH), 10.74 (s, 1H, NH), 8.41 (d, *J* = 8.3 Hz, 1H), 8.19 (d, *J* = 8.3 Hz, 1H), 8.01 (d, *J* = 7.8 Hz, 1H), 7.78 (d, *J* = 7.8 Hz, 1H), 7.73 (d, *J* = 8.4 Hz, 2H), 7.56 (dd, *J* = 16.0, 8.2 Hz, 3H), 7.41 (t, *J* = 7.8 Hz, 1H), 7.22 (dt, *J* = 21.9, 7.5 Hz, 2H), 7.09 (d, *J* = 1.8 Hz, 1H), 6.94 (d, *J* = 9.0 Hz, 1H), 6.70 (dd, *J* = 9.0, 2.1 Hz, 1H), 3.85 (s, 2H), 3.72 (s, 3H), 2.31 (s, 3H); ^{13}C NMR**;** 170.0 (carboxylic C=O) , 169.1 (amidic C=O) and 168.3 (amidic C=O) , 166.9 , 156.0 , 140.5 , 139.0 , 138.1 , 136.7 , 134.5 , 134.1 , 132.9 , 131.7 , 131.5 , 131.1 , 131.0 , 129.4 , 127.8 , 123.9 , 123.1 , 121.6 , 121.1 , 118.2 , 115.1 , 113.0 , 112.0, 102.0 , 57.0, 54.8, 35.2, 33.0 ; Anal. Calcd. for $C_{33}H_{26}ClN_3O_6$: C, 66.50; H, 4.40; N, 7.05. Found: C, 66.33; H, 4.57; N, 7.38.

2-(2-(2-Chloroacetamido)benzamido) benzoic acid 5m[17]

White crystals (ethanol 95%); yield (0.57 g, 85%); m.p. (223-224.5^{o}C); FT-IR: 3120 (sp^2 C-H); 2500-3500 (broad band COOH); 1688 (carboxylic C=O), 1658 (amidic C=O); 1255 (C-O);747 (o-di-substituted benzene); ^{1}H NMR**;** 13.63 (s, 1H, COOH), 11.92 (s, 1H, NH), 11.19 (s, 1H, NH), 8.57 (d, *J* = 8.3 Hz, 1H), 8.28 (d, *J* = 8.3 Hz, 1H), 8.06 (d, *J* = 7.9 Hz, 1H), 7.88 (d, *J* = 7.8 Hz, 1H,), 7.65-7.3 (m, 4H), 4.37 (s, 2H); ^{13}C NMR; 170.0 (carboxylic C=O) , 166.8 (amidic C=O) and 165.4 (amidic C=O) , 140.4 , 137.9 , 134.5 , 132.8 , 131.6 , 128.3 , 124.7 , 124.4 , 123.9 , 122.4 , 121.2, 118.2 , 43.4; Anal. Calcd. for $C_{16}H_{13}ClN_2O_4$:C, 57.75; H, 3.94; N, 8.42. Found: C, 57.94; H, 4.12; N, 8.38.

2-(2-Acetamidobenzamido) benzoic acid 5n[13]

To an aqueous solution of compound **3** (0.512 g, 0.002 mol, dissolved in 1.5 ml conc. HCl in 50 ml distilled water), 2 ml acetic anhydride was added, the aqueous mixture was then directly added to an ice-cooled solution of sodium acetate (2.5 g in 25 ml distilled water), the mixture was stirred in an ice bath till crystals of the product were formed, the product was filtered off, dried at 45 °C.
White crystals (ethanol 95%); yield (0.52 g, 90%); m.p. (215-216^{o}C, no m.p. available in reference **[13]**); FT-IR**,** 3129 (sp^2 C-H), 2911(sp^3 C-H), 2500-3000, (broad band COOH), 1690 (carboxylic C=O), 1655 (amidic C=O), , 1230 (C-O**);** ^{1}HNR and ^{13}CNMR data are in agrement with published data. Anal. Calcd. for $C_{16}H_{14}N_2O_4$: C, 64.42; H, 4.73; N, 9.39. Found: C, 64.22; H, 4.55; N, 9.30.

General method for the synthesis of N-(2-(4-oxo-4*H*-benzo[d][1,3] oxazin-2-yl)phenyl) acyl amides (6a-n): [18]

To each of the compounds 5a-n (0.01 mol), was added acetic anhydride (5 ml) and the mixture was refluxed for 15 minutes, or till suspension turned in solution monitoring the reaction by TLC (using a mixture of chloroform-methanol 9:1). After cooling the solution, the precipitate was filtered and dried at 45 °C.

N-(2-(4-oxo-4*H*-benzo[d][1,3]oxazin-2-yl) phenyl) benzamide 6a[19]

Yellow crystals (n-butanol-ethanol 4:1); yield (0.313 g, 91.6%); m.p. (172.5-173.5^{o}C), reported (173-174); FT-IR: 3065 (sp^{2}C-H); 3566 (amidic NH); 1716 (lactone C=O);1671 (amidic C=O); 1220 (C-O);761 (*o*-disubstituted benzene); ^{1}H NMR**;** 12.65 (s, 1H,NH), 8.71 (d, *J* = 8.4 Hz, 1H), 8.12 (dd, *J* = 7.8, 1.2 Hz, 1H), 8.06 (dd, *J* = 8.1, 1.4 Hz, 1H), 8.03 – 7.92 (m, 3H), 7.73 – 7.56 (m, 5H), 7.50 (d, *J* = 8.0 Hz, 1H), 7.31 – 7.22 (m, 1H); ^{13}C NMR**;** 165.7 (amidic C=O) , 158.5 (lactone C=O) , 157.3 (C=N) , 145.4 , 140.0 , 137.6 , 135.4 , 134.1 , 132.8 , 129.9 , 129.5, 129.4 , 128.7 , 127.7, 126.0, 123.8 , 120.8 , 117.2, 116.9; Anal. Calcd. for $C_{21}H_{14}N_2O_3$: C, 73.68; H, 4.12; N, 8.31. Found: C, 73.54; H, 4.31; N, 8.32.

4-Chloro-N-(2-(4-oxo-4*H*-benzo[d][1,3] oxazin-2-yl)phenyl)benzamide 6b

White crystals (n-butanol-ethanol 4:1); yield (0.305 g, 81%); m.p. (208.5-209.5 ^{o}C); FT-IR : 1767 (lactone C=O); 1677 (amidic C=O); 1221 (C-O); 757 (*o*-disubstituted benzene); 845 (*p*-disubstituted benzene); ^{1}H NMR**;** 12.56 (s, 1H,NH), 8.67 (d, *J* = 8.4 Hz, 1H), 8.17 (dd, *J* = 7.8, 1.2 Hz, 1H), 8.12 (dd, *J*

= 8.1, 1.4 Hz, 1H), 8.06 – 7.99 (m, 3H), 7.74 (d, *J* = 8.5 Hz, 2H), 7.70 – 7.63 (m, 2H), 7.59 (d, *J* = 8.1 Hz, 1H), 7.36 – 7.29 (m, 1H); ^{13}C NMR**;** 164.6 (amidic C=O) , 158.6 (lactone C=O) , 157.3 (C=N) , 145.4 , 139.6 , 137.8 , 137.6 , 134.0 , 134.0 , 130.0 , 129.6 , 129.5 , 129.5, 128.7 , 126.3 , 124.1 , 121.2 , 117.6, 117.2; Anal. Calcd. for $C_{21}H_{13}ClN_2O_3$: C, 66.94; H, 3.48; N, 7.43. Found: C, 66.66; H, 3.45; N, 7.33.

4-Methyl-N-(2-(4-oxo-4*H*-benzo[d][1,3] oxazin-2yl)phenyl)benzamide 6c:[19]

White crystals (n-butanol-ethanol 4:1); yield (0.292g, 82%) ; m.p. (183-184 ^{o}C); FTIR:1767 (lactone C=O); 1686 (amidic C=O); 1220 (C-O); 744 (*o*-disubstituted benzene); 841 (*p*-disubstituted benzene; ^{1}H NMR**;** 12.63 (s, 1H,NH), 8.76 (s, 1H), 8.16 (d, *J* = 9.6 Hz, 2H), 7.99-7.64 (m, 8H), , 7.31 (s, 1H), 2.44 (s, 3H); ^{13}C NMR**;** 171.1 (amidic C=O), 158.5 (lactone C=O) , 156.9 (C=N) , 145.7, 141.0 , 139.5 , 137.1 , 133.4 , 129.9 , 129.4 , 128.7 , 128.5 , 126.9 , 126.4 , 123.6 , 121.6 , 117.7, 117.2, 31.0; Anal. Calcd. for $C_{22}H_{16}N_2O_3$: C, 74.15; H, 4.53; N, 7.86. Found: C, 73.96; H, 4.7; N, 8.13.

2-(4-Methoxyphenyl)-N-(2-(4-oxo-4*H*-benzo [d][1,3] oxazin-2-yl)phenyl) acetamide 6d

White crystals (n-butanol-ethanol 4:1); yield (0.303g, 78.5%); m.p. (185-186.5 ^{o}C); FT IR: 3648 (NH); 3078, 3011 (sp^2 C-H); 2928,2843 (sp^3 C-H); 1767 (lactone C=O); 1686 (amidic C=O); 1219 (C-O); 766 (o-di-substituted benzene); 818 (p-di-substituted benzene); ^{1}H NMR**;** 11.78 (s, 1H,NH), 8.45 (d, *J* = 7.8 Hz, 1H), 8.17 (dd, *J* = 7.8, 0.9 Hz, 1H), 8.05 (dd, *J* = 8.0, 1.4 Hz, 1H), 8.02 – 7.95 (m, 1H), 7.71 – 7.57 (m, 3H), 7.33 – 7.23 (m, 3H), 6.91 – 6.85 (m, 2H), 3.78 (s, 2H), 3.71 (s, 3H, ; ^{13}C NMR**;** 170.3 (amidic C=O), 158.8 (lactone C=O), 158.6 (C=N) , 157.1 , 145.6 , 139.5 , 137.3 , 133.7 , 130.7 , 129.9 , 129.4 , 128.4 , 127.5 , 127.1 , 123.7 , 121.3 , 117.5 , 117.2, 114.3 , 55.4, 43.7; Anal. Calcd. for $C_{23}H_{18}N_2O_4$: C, 71.49; H, 4.7; N, 7.25. Found: C, 71.63; H, 4.62; N, 7.49.

N-(2-(4-oxo-4*H*-benzo[d][1,3] oxazin-2-yl) phenyl)-3-phenylpropanamide 6e

Yellow crystals (n-butanol-ethanol 4:1); yield (0.242 g, 65.5%) m.p. (159-160); FT-IR: 3062,3022 (sp^2 C-H); 2959, 2928 (sp^3 C-H); 1773 (lactone C=O);1686 (amidic C=O); 1218 (C-O); 751 (*o*-disubstituted benzene); ^{1}H NMR**;** 11.58 (s, 1H,NH), 8.40 (dd, *J* = 8.4, 0.9 Hz, 1H), 8.18 (dd, *J* = 7.9, 1.2 Hz, 1H), 8.07 – 7.95 (m, 2H), 7.75 (d, *J* = 7.6 Hz, 1H), 7.70 – 7.56 (m, 2H), 7.31 – 7.10 (m, 6H), 2.98 (t, *J* = 7.5 Hz, 2H), 2.80 (t, *J* = 7.5 Hz, 2H); ^{13}C NMR, 171.1 (amidic C=O), 158.8 (lactone C=O), 157.1 (C=N), 145.7, 141.2, 139.3, 137.4, 134.2, 133.7, 129.9, 129.4, 128.7, 128.7, 127.0, 126.4, 123.7, 121.5, 117.7, 117.2, 31.3; Anal. Calcd. for $C_{23}H_{18}N_2O_3$: C, 74.58; H, 4.9; N, 7.56. Found: C, 74.32; H, 4.85; N, 7.72.

2-(Naphthalen-1-yl)-N-(2-(4-oxo-4H-benzo [d][1,3] oxazin-2-yl)phenyl) acetamide 6f

Yellow crystals (n-butanol-ethanol 4:1); yield (0.305 g, 75%); m.p. (202-203 ^{o}C); FT-IR: 3236 (amidic NH); 3066,3038 (sp^2 C-H); 1772 (lactone C=O); 1682 (amidic C=O); 1247C-O); 747 (*o*-disubstituted benzene); ^{1}H NMR**;** 11.76 (s, 1H,NH), 8.40 (d, *J* = 7.7 Hz, 1H), 8.21 – 8.11 (m, 2H), 8.04 (dd, *J* = 8.0, 1.5 Hz, 1H), 8.00 – 7.91 (m, 2H), 7.86 (d, *J* = 8.2 Hz, 1H), 7.71 – 7.64 (m, 2H), 7.63 – 7.56 (m, 2H), 7.55 – 7.45 (m, 3H), 7.31 – 7.25 (m, 1H), 4.36 (s, 2H); ^{13}C NMR**;** 170.0 (amidic C=O), , 158.8 (lactone C=O) , 157.1 (C=N), 145.6 , 139.3 , 137.3 , 133.8 , 133.6 , 132.4 , 132.1 , 130.0 , 129.4 , 128.9 , 128.7 , 128.4 , 128.0 , 127.1 , 126.7 , 126.2, 126.0 ,124.5 , 123.8, 121.5 ,117.9, 117.2, 42.2 ; Anal. Calcd. for $C_{26}H_{18}N_2O_3$**:** C, 76.83; H, 4.46; N, 6.89. Found: C, 76.60; H, 4.43; N, 7.12.

2-(2,4-Dichlorophenyl)-N-(2-(4-oxo-4H-benzo[d][1,3] oxazin-2-yl) phenyl) acetamide 6g

White crystals (n-butanol-ethanol 4:1); yield (0.31 g, 73%); m.p. (218-220 ^{o}C); FT-IR: 3150 (sp^2 C-H), 2890 (sp^3 C-H); 1770 (lactone C=O); 1670 (amidic C=O); 1235 (C-O); ^{1}H NMR**;** 11.87 (s, 1H, NH), 8.37 (d, *J* = 7.9 Hz, 1H), 8.22 – 8.17 (m, 1H), 8.08 (dd, *J* = 8.0, 1.4 Hz, 1H), 8.04 – 7.97 (m, 1H), 7.79 (d, *J* = 7.9 Hz, 1H), 7.71 – 7.60 (m, 3H), 7.52 (d, *J* = 8.3 Hz, 1H), 7.43 (dd, *J* = 8.2, 2.1 Hz, 1H), 7.31 (t, *J* = 7.7 Hz, 1H), 4.05 (s, 2H); ^{13}C NMR; 166.9 (amidic C=O), 157.0 (lactone C=O); 156.5 (C=N), 144.2, 139.3, 135.3, 134.0, 133.1, 133.0, 131.5, 130.0, 128.5, 128.3, 127.9, 126.5, 125.7, 125.2, 122.2, 119.8, 115.7, 114.0, 41.4;

Anal. Calcd. for $C_{22}H_{14}Cl_2N_2O_3$: C, 62.13; H, 3.32; N, 6.59. Found: C, 62.39; H, 3.44; N, 6.81.

N-(2-(4-oxo-4H-benzo[d][1,3] oxazin-2-yl)phenyl)hexanamide 6h

White crystals (n-butanol-ethanol 4:1); yield (0.181 g, 54%); m.p. (117.5-119.5 ^oC); FT-IR: 3178,3112 (sp^2C-H); 2951 ,2928, 2865 (sp^3C-H);1774 (lactone C=O); 1692 (amidic C=O); 1220 (C-O); 749 (*o*-disubstituted); ^1H NMR **;** 11.66 (s, 1H,NH), 8.43 (dd, *J* = 8.3, 0.7 Hz, 1H), 8.17 (dd, *J* = 7.8, 1.2 Hz, 1H), 8.09 – 7.97 (m, 2H), 7.74 (d, *J* = 7.8 Hz, 1H), 7.70 – 7.57 (m, 2H), 7.31 – 7.23 (m, 1H), 2.47 (t, *J* = 7.4 Hz, 2H), 1.67 (m, *J* = 7.3 Hz, 2H), 1.36 – 1.30 (m, 4H), 0.89 – 0.84 (m, 3H); ^{13}C NMR**;** 171.9 (amidic C=O) , 158.7 (lactone C=O) , 157.3 (C=N), , 145.7 , 139.6 , 137.4 , 133.7 , 129.9 , 129.4 , 128.5 , 126.8 , 123.5 , 117.4, 117.2, 37.9 , 31.3 , 25.2, 22.3 , 14.3; Anal. Calcd. for $C_{20}H_{20}N_2O_3$: C, 71.41; H, 5.99; N, 8.33. Found: C, 71.68; H, 6.12, N, 8.21.

N-(2-(4-oxo-4*H*-benzo[d][1,3]oxazin-2-yl)phenyl)nicotinamide 6i

White crystals (n-butanol-ethanol 4:1); yield (0.256 g, 74.5 %) m.p. (199.5-202^{o}C);FT-IR:3685(amidic NH);3175(sp^2C-H);1770(lactone C=O); 1688(amidic C=O);1220(C-O); 741(o-di-substituted benzene); ^1H NMR**;** 12.49 (s, 1H,NH), 9.24 (s, 1H,), 8.86 (d, *J* = 4.5 Hz, 1H), 8.65 (d, *J* = 8.3 Hz, 1H), 8.37 (d, *J* = 7.9 Hz, 1H), 8.18 (dd, *J* = 15.4, 7.9 Hz, 2H), 8.01 (t, *J* = 7.7 Hz, 1H), 7.74 – 7.64 (m, 3H), 7.59 (d, *J* = 8.1 Hz, 1H), 7.37 (t, *J* = 7.7 Hz, 1H); ^{13}C NMR**;** 164.3 (amidic C=O), 158.5 (lactone C=O) , 157.4 (C=N), 153.2 , 148.7 , 145.4 ,139.3 ,137.4 , 135.6 , 133.9 , 131.1 , 130.0 , 129.5 , 128.7 , 126.1 , 124.4 , 121.6 , 118.0 , 117.2; Anal. Calcd. for $C_{20}H_{13}N_3O_3$: C, 69.96; H, 3.82; N, 12.24. Found: C, 70.13; H, 3.96; N, 12.01.

N-(2-(4-oxo-4*H*-benzo[d][1,3]oxazin-2-yl) phenyl) pentanamide 6j

White crystals (n-butanol-ethanol 4:1); yield (0.235 g, 73%); m.p. (128.5-130 ^oC); FT-IR: 3174, 3113 (sp^2 C-H); 2956, 2869 (sp^3 C-H); 1771 (lactone C=O); 1680 (amidic C=O); 1218 (C-O); 751 (*o*-disubstituted benzene; ^1H NMR; 11.59 (s, 1H, NH), 8.45 (d, *J* = 8.4 Hz, 1H), 8.19 (d, *J* = 7.8 Hz, 1H), 8.07 (d, *J* = 8.0 Hz, 1H), 8.01 (t, *J* = 7.7 Hz, 1H), 7.75 (d, *J* = 8.1 Hz, 1H), 7.64 (dt, *J* = 25.4, 7.8 Hz, 2H), 7.27 (t, *J* = 7.6 Hz, 1H), 2.48 (d, *J* = 7.4 Hz, $2H_2$), 1.75 – 1.62 (m, 2H), 1.48 – 1.34 (m, 2H), 0.92 (t, *J* = 7.3 Hz, 3H); ^{13}C NMR**;** 171.9 (amidic C=O), 158.7 (lactone C=O) , 157.3 (C=N), 145.7 , 139.7 , 137.4 , 133.6 , 129.9 , 129.4 , 128.5, 126.8 , 123.5 , 121.3 , 117.5, 117.2 , 37.7 , 27.6, 22.2 , 14.1; Anal. Calcd. for $C_{19}H_{18}N_2O_3$: C, 70.79; H, 5.63; N, 8.69. Found: C, 71.12; H, 5.84; N, 8.75.

3, 4,5-Trimethoxy-N-(2-(4-oxo-4*H*-benzo [d][1,3] oxazin-2-yl)phenyl) benzamide 6k

White crystals (n-butanol-ethanol 4:1); yield (0.337 g, 78%); m.p. (216.5-217.5 ^oC); FT-IR: 3064, 3004 (sp^2 C-H); 2967, 2838 (sp^3 C-H); 1774 (lactone C=O); 1680 (amidic C=O); 1219 (C-O); 754 (*o*-disubstituted benzene); ^1H NMR**;** 12.18 (s, 1H, NH), 8.62 (d, *J* = 8.3 Hz, 1H), 8.17 (dd, *J* = 20.5, 7.8 Hz, 2H), 7.98 (t, *J* = 7.6 Hz, 1H), 7.69 (dt, *J* = 14.8, 7.5 Hz, 2H), 7.49 (d, *J* = 8.0 Hz, 1H), 7.36 (t, *J* = 7.7 Hz, 1H, 7.29 (s, 2H), 3.82 (s, 6H,), 3.80 (s, 3H); ^{13}C NMR**;** 170.1 (amidic C=O), 167.30 (lactone C=O) , 164.9 (C=N), 153.3 , 141.1 140.9 , 138.9 , 132.9 , 131.6 , 130.3 , 128.4 , 124.6 , 124.5 , 123.9 , 122.6 , 121.1 , 118.1, 105.3, 60.6, 56.4; Anal. Calcd. for $C_{24}H_{20}N_2O_6$:C, 66.66; H, 4.66; N, 6.48. Found: C, 66.83; H, 4.59; N, 6.72.

2-(1-(4-Chlorobenzoyl)-5-methoxy-2-methyl-1*H*-indol-3-yl)-N-(2-(4-oxo-4*H*-benzo[d][1,3] oxazin-2-yl) phenyl) acetamide 6l

Yellow crystals (n-butanol-ethanol 4:1); yield (0.416 g, 72%) ; m.p. (183-185 ^oC); FT-IR:3647 (amidic NH); 3094 (sp^2 C-H);2923,2831 (sp^3 C-H);1772 (lactone C=O); 1683 (amidic C=O); 1219 (C-O); 751 (*o*-disubstituted benzene); ^1H NMR**;** 11.54 (s, 1H,NH), 8.43 (d, *J* = 8.3 Hz, 1H), 8.15 (d, *J* = 7.7 Hz, 1H), 8.06 (d, *J* = 7.9 Hz, 1H), 7.85 (t, *J* = 7.6 Hz, 1H), 7.69 – 7.55 (m, 6H), 7.37 (d, *J* = 8.0 Hz, 1H), 7.30 (t, *J* = 7.6 Hz, 1H), 7.12 (s, 1H), 6.89 (d, *J* = 8.9 Hz, 1H), 6.71 (d, *J* = 8.9 Hz, 1H), 3.97 (s, 2H), 3.67 (s, 3H), 2.27 (s, 3H); ^{13}C NMR**;** 169.4 (amidic C=O) , 168.2 (lactone C=O) , 158.7 (C=N), 157.1 , 156.1 , 145.6 , 139.2 , 138.1, 137.2 , 136.2 , 134.5 , 133.5 , 131.5 , 131.2 , 130.9 , 130.0 , 129.4 , 129.3 , 128.4 , 126.9 , 123.9 , 121.8 , 118.3 , 117.1 , 115.0 , 113.6 , 111.9, 102.1 , 57.7, 54.6, 35.0, 32.2 , 15.5, 12.7; Anal. Calcd. for

$C_{33}H_{24}ClN_3O_5$: C, 68.57; H, 4.19; N, 7.27. Found: C, 68.8; H, 4.36; N, 7.59.

2-Chloro-N-(2-(4-oxo-4*H*-benzo[d][1,3] oxazin-2-yl)phenyl)acetamide 6m

White crystals (n-butanol-ethanol 4:1); yield (0.276 g, 88%); m.p. (180.5-182 oC); FT-IR: 3164 (sp2 C-H); 2967, 1768 (lactone C=O);1693 (amidic C=O); 1220 (C-O); 744 (*o*-disubstituted benzene); 1H NMR; 12.31 (s, 1H,NH), 8.56 (d, J = 8.4 Hz, 1H), 8.17 (dd, J = 20.3, 7.9 Hz, 2H), 8.02 (t, J = 7.7 Hz, 1H), 7.84 (d, J = 8.1 Hz, 1H), 7.68 (dd, J = 11.3, 7.4 Hz, 2H), 7.35 (t, J = 7.7 Hz, 1H, Ar-H), 4.54 (s, 2H); 13C NMR; 165.9 (amidic C=O) , 158.5 (lactone C=O) , 156.8(C=N) , 145.6 , 138.9 , 137.7 , 133.9 , 129.9 , 129.5 , 128.6 , 126.8 , 124.4 , 121.1 , 117.6, 117.3, 43.9; Anal. Calcd. for $C_{16}H_{11}ClN_2O_3$:C, 61.06; H, 3.52; N, 8.90. Found: C, 61.23; H, 3.38; N, 8.81.

N-(2-(4-oxo-4*H*-benzo[d][1,3] oxazin-2-yl)phenyl)acetamide 6n[19]

White crystals (n-butanol-ethanol 4:1); yield (0.475 g, 85%); m.p. (213-214.5 ^{o}C); FT-IR; 3152 (sp^2 C-H); 2960 (sp^3 C-H), 1766 (lactone C=O); 1690 (amidic C=O); ^{1}H NMR; 11.69 (s, 1H), 8.74 – 6.99 (m, 8H), 2.22 (s, 3H; ^{13}C NMR**;** 168.6 (amidic C=O), 158.0 (lactone C=O), 157.5 (C=N), 145.2 , 140.8, 136.6 , 134.2, 129.4 , 128.9, 128.8, 126.1, 122.7, 120.5, 116.7, 114.3, 25.8 ; Anal. Calcd. for $C_{16}H_{12}N_2O_3$: C, 68.56; H, 4.32; N, 9.99. Found: C, 68.43; H, 4.23; N, 9.76.

***Docking studies of the proposed compounds (5a-n) and (6a-n) with W HIV-1 RT*.**

The 2D models of the proposed compounds were constructed using the program ChemDraw and then copied into the MOE (version 2019.0101) software interface, where the energies of the proposed compounds were minimized to obtain the most stable conformers, which were then saved as a database for use in the docking calculations. The X-ray crystallographic structure of the RT enzyme co-crystallized with nevirapine (PDB ID: 4PUO) was obtained from the protein databank, validated for docking (rmsd = 0.21 Å), and then prepared for docking. Docking simulations were performed using the MOE docking application employing Triangle Matcher as the placement scheme, rigid receptor as the refinement scheme, London ΔG as the scoring function, and GBVI/WSA dG as the refinement score. The active site was selected as the pocket where the ligand was present, and docking was performed in the presence of the nevirapine ligand.

***Enzymatic HIV-1 RTI Assay.* [20]**

Recombinant HIV-1-RT (4–6 ng) diluted in lysis buffer (20 µL per well) was used. In a separate reaction, lysis buffer with no HIV-1-RT was used as a negative control. Then, 20 µL of RT inhibitor diluted in lysis buffer was incubated with 20 µL of reaction mixture per reaction tube for 1 h at 37 °C. Sufficient foil bags for the number of MP modules were opened and used. The MP modules are then put into the frame in the correct orientation. MP modules were deemed as ready to be used and did not need to be rehydrated prior to the addition of the samples. The samples (60 µL) were transferred into the wells of the MP modules and covered with a cover foil before being incubated for 1 h at 37 °C. The solution was then completely removed before each well was rinsed five times with 250 µL of washing buffer for 30 s, which was then carefully removed. Diluted anti-IG-POD (200 µL, 200 Mu/mL) was added to each well; then, the MP modules were covered with a cover foil and incubated for 1 h at 37 °C. The solution was then completely removed, and each well was rinsed five times using 250 µL of washing buffer for 30 s, which was then carefully removed. ABTS substrate solution (200 µL) was added to each well, which was then incubated at +15 °C to +25 °C until the color of the solutions (green color) was sufficient for photometric detection (10–30 min). The absorbance of the samples was measured using a microplate (ELISA) reader, at 450 nm (reference wavelength of approximately 490 nm).

***In vitro determination of cytotoxicity of 5a, 6d, 6h, and 6k* [21]**

Chemicals used in cytotoxicity assay: Dimethyl sulfoxide (DMSO), crystal violet, and trypan blue dye were purchased from Sigma (St. Louis,follo Mo., USA). Fetal Bovine serum, DMEM, HEPES buffer solution, L-glutamine, gentamycin, and 0.25% Trypsin-EDTA were purchased from Lana.

The mammalian cell line used, HeLa cells (human cervical carcinoma), were obtained

from the VACSERA tissue culture unit. For cell line propagation, cells were propagated in Dulbecco's modified Eagle's medium supplemented with 10% heat-inactivated fetal bovine serum, 1% L-glutamine, HEPES buffer, and 50 µg mL^{-1} gentamycin. All cells were maintained at 37 °C in a humidified atmosphere with 5% CO_2 and were subcultured twice a week.

The crystal violet stain (1%) - was composed of 0.5% (w/v) crystal violet and 50% methanol and then made up to volume with double-distilled H_2O and filtered through a Whatman No.1 filter paper.

The assayProcedure[21]- Cytotoxicity evaluation was carried out using viability assay. The cells were seeded in a 96-well plate at a cell concentration of 1×10^4 cells per well in 100 µL of growth medium. A fresh medium containing different concentrations of the test sample was added after 24 h of seeding. Serial twofold dilutions of the tested chemical compounds were added to confluent cell monolayers dispensed into 96-well, flat-bottomed microtiter plates (Falcon, NJ, USA) using a multichannel pipette. The microtiter plates were incubated at 37 °C in a humidified incubator with 5% CO_2 for a period of 24 h. Three wells were used for each concentration of the test sample. Control cells were incubated without a test sample and with or without dimethyl sulfoxide (DMSO). The small percentage of DMSO present in the wells (maximum of 0.1%) was found not to affect the experiment. After incubation of the cells at 37 °C for 24 h, the viable cell yield was determined using a colorimetric method.

In brief, after the end of the incubation period, the solvent media were aspirated and crystal violet solution (1%) was added to each well for at least 30 min. The stain was removed, and the plates were rinsed using tap water until all excess stain was removed. Glacial acetic acid (30%) was then added to all of the wells and mixed in thoroughly, and then, the absorbance of the plates was measured after gentle shaking on a microplate reader (TECAN, Inc.) at a test wavelength of 490 nm. All results were corrected for background absorbance detected in wells without added stain. Treated samples were compared with the cell control in the absence of the tested compounds. All experiments were carried out in triplicate. The cell cytotoxicity effects of each tested compound were calculated. The optical density was measured using a microplate reader (Sunrise, TECAN, Inc., USA) to determine the number of viable cells, and the percentage of viability was calculated using $[(OD_t/OD_c)] \times 100\%$, where OD_t is the mean optical density of wells treated with the test samples and OD_c is the mean optical density of untreated cells. The relationship between the surviving cells and drug concentration was plotted to obtain the survival curve of each tumor cell line after treatment with the specified compound. The 50% inhibitory concentration (IC_{50}), the concentration required to cause toxic effects in 50% of intact cells, was estimated from plots of the dose-response curve for each concentration using GraphPad Prism software (San Diego, CA, USA).

RESULTS AND DISCUSSION

Synthesis

Three generations of N-acylanthranoylanthranilic acids were synthesized and tested for inhibition of adenovirus replication activity by Öberg et al. [13] Starting from the amides, obtained from N-protected and activated carboxyl of anthranilic acid by oxalyl chloride coupled to ethyl anthranilate, were N-acylated by the suitable acid chloride after N-deprotection and ester hydrolysis. An example of the synthesis of N-benzoyl and N-acetyl compounds is illustrated in Scheme 1.

The targeted compounds (5a-n) and (6a-n) were synthesized *via* the route shown in Scheme 2. The key intermediate (3) was prepared *via* the reaction of isatoic anhydride (1) with anthranilic acid (2) in presence of sodium hydroxide at 55°C[22] The newly synthesized N-acylanthranoylanthranilic acid derivatives (5b, d, e-l) and the reported ones (5a, c, and n)[13], (5i chemical structure characterization data can not accessible) [16], and (5m)[17] were obtained in 60-90 % yield *via* acylation of (3) by alkyl-, aralkyl-, and aryl acid chlorides (4a-m) and by acetic anhydride (4n). The acid chlorides were prepared by the conventional reaction of thionyl chloride and the assigned carboxylic acids.[14]

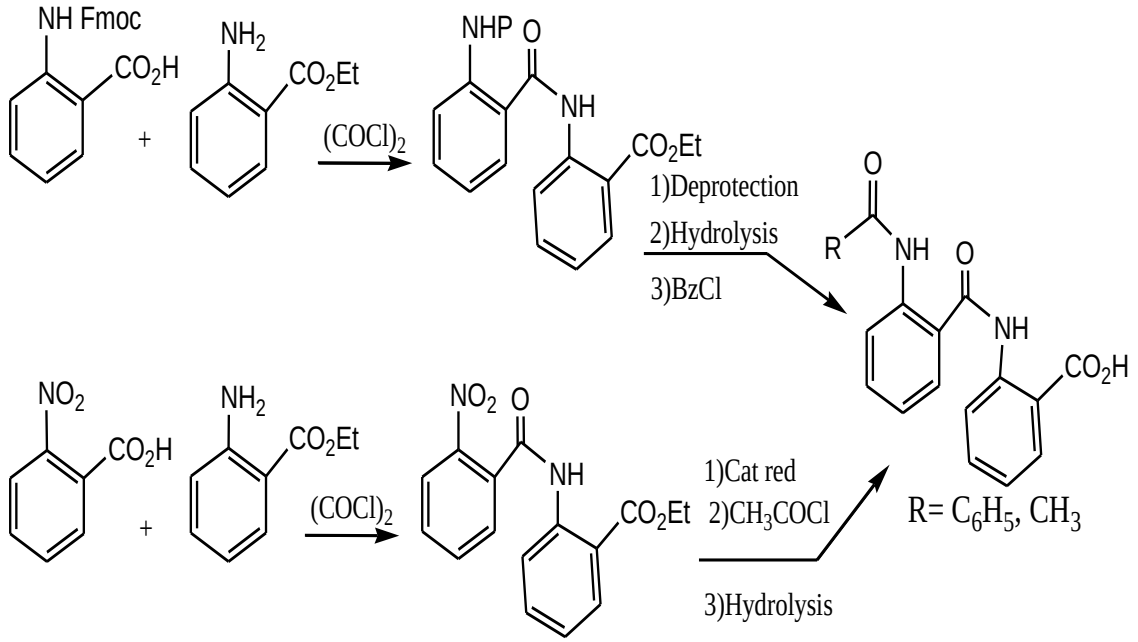

Scheme 1: Routes of synthesis of selected N-acylanthranoylanhranilic acids[13]

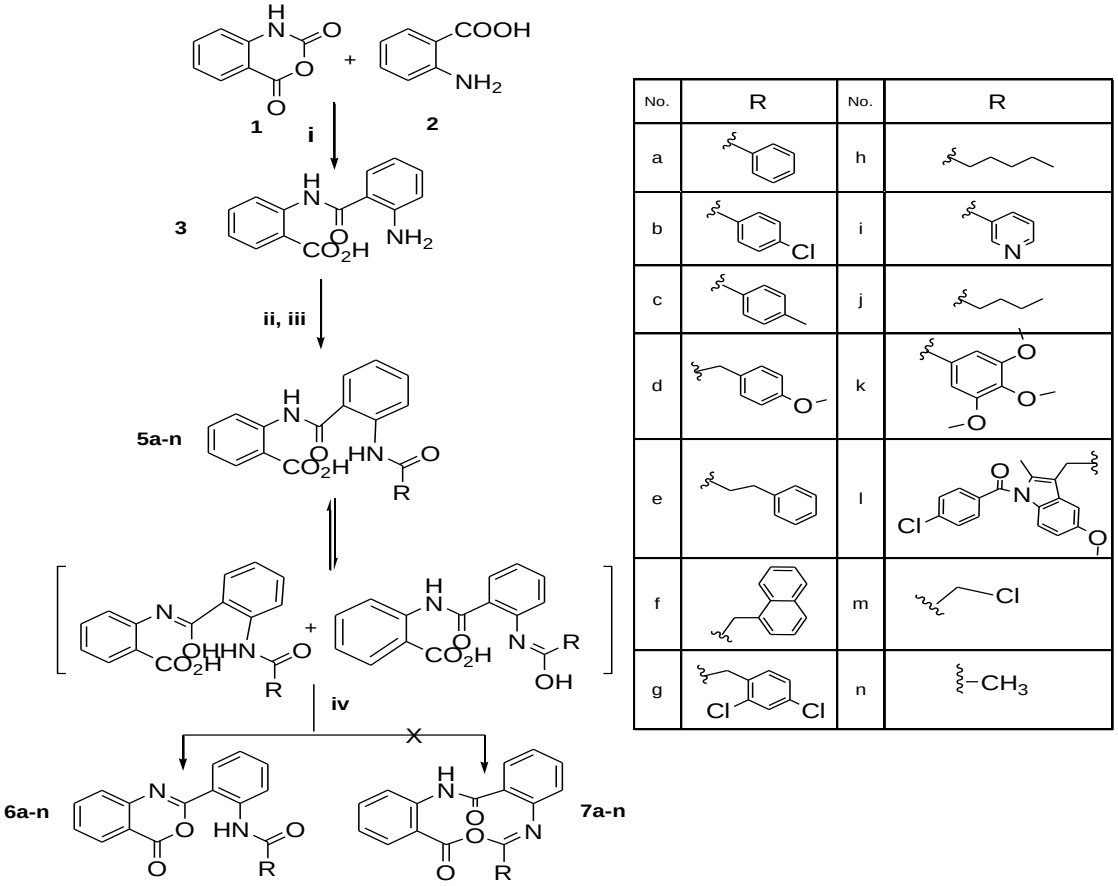

No.	R	No.	R
a		h	
b	Cl	i	N
c		j	
d	O	k	O, O, O
e		l	O, N, Cl, O
f		m	Cl
g	Cl, Cl	n	CH3

i) NaOH, 55 °C 1.5 h or till clear **ii) 4a-m** RCOCl (1eq), rt, dioxane, **iii) 4n** $(Ac)_2O$, AcONa, 0-5 °C; **iv)** $(Ac)_2O$, reflux, 15 min

Scheme 2: Synthesis of the targeted compounds **5a-n** and **6a-n**

Synthesis of 2-substituted 4*H*-benzo[d] 1,3- oxazin-4-one derivatives was reviewed by Coppola[15] using anthranilic acid or isatoic anhydride under different reaction conditions. Annor-Gyamfi and Bunce[23] explored the reaction of substituted anthranilic acid in presence of excess ortho acids under thermal and microwave conditions which yielded in some cases the dihydro derivative.

Three compounds, (6a, 6c, and 6n) were previously reported by Kimmich et al[19] by means of N-acylation of 2-(2-aminophenyl)-4*H*-benzo[d]1,3-oxazin-4-one with the appropriate acid chloride, however, structures were not adequately characterized. In this study, benzoxazinones (6a-n) were obtained in 54- 91.6 % yield via the cyclo-dehydration of (5a-n) by heating to reflux with acetic anhydride according to the procedure previously reported by El-Hashash et al.[18] However, there were still questions remaining about these structure assignments. Therefore, to resolve the controversy about the molecular structures of the compounds, hetero-nuclear multiple bond correlation (HMBC) spectroscopy was used to reveal that in 6c H2" couples to amidic carbonyl C7" and H6' couples to the carbon of imine C2. Figure 3 shows the proposed formation of a six-membered benzoxazinone ring. Unequivocal evidence for the structure of N-(2-(4-oxo-4*H*-benzo[d][1,3] oxazine-2-yl) phenyl) benzamide (6a), came from single-crystal X-ray diffraction Figure 4 and the refined data listed in Table S2. The central aniline nucleus (N1-C8-C13) is attached to the benzoyl group through (C8-N1) *ortho*-to the six-membered 6H-1,3-oxazinone-6-one nucleus linked to the aniline motif through (C14-C13) and fused to the benzene ring through (C16-C17). The plots revealed the "Butterfly-like" Sconformation typical for most NNRTIs[24].

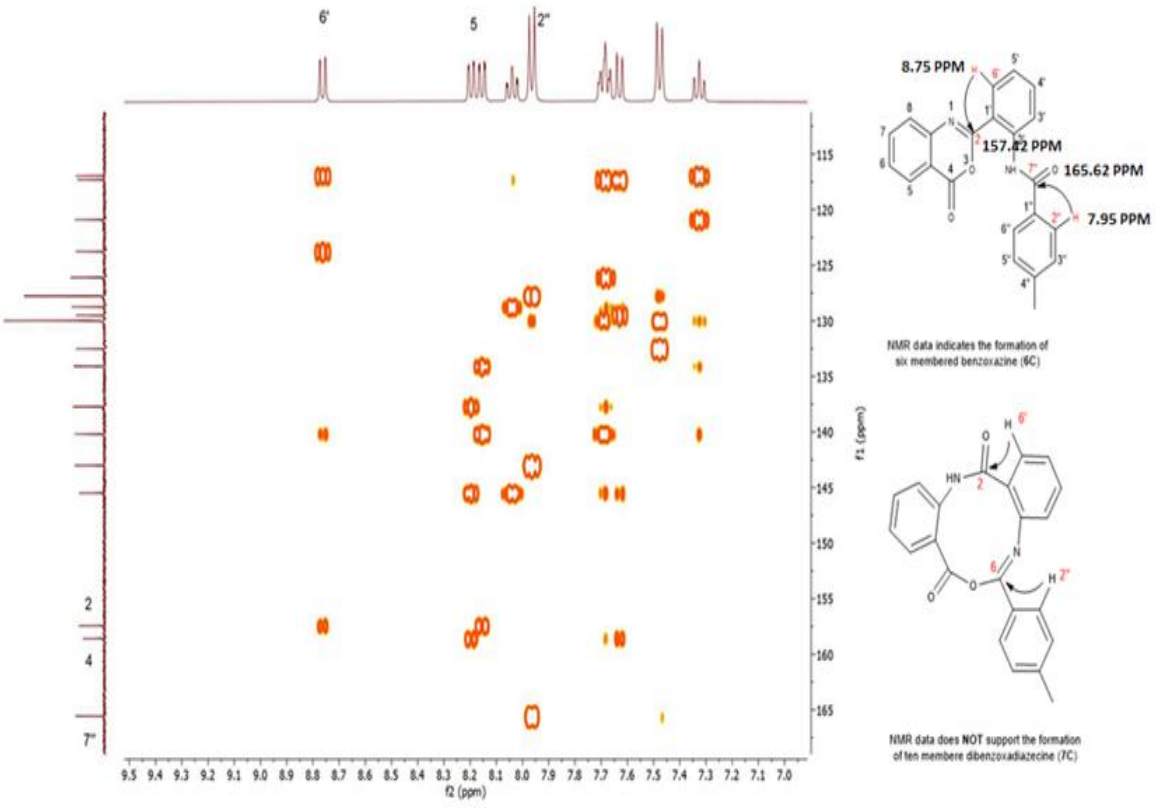

Fig. 3: HMBC spectrum of compound **6c**

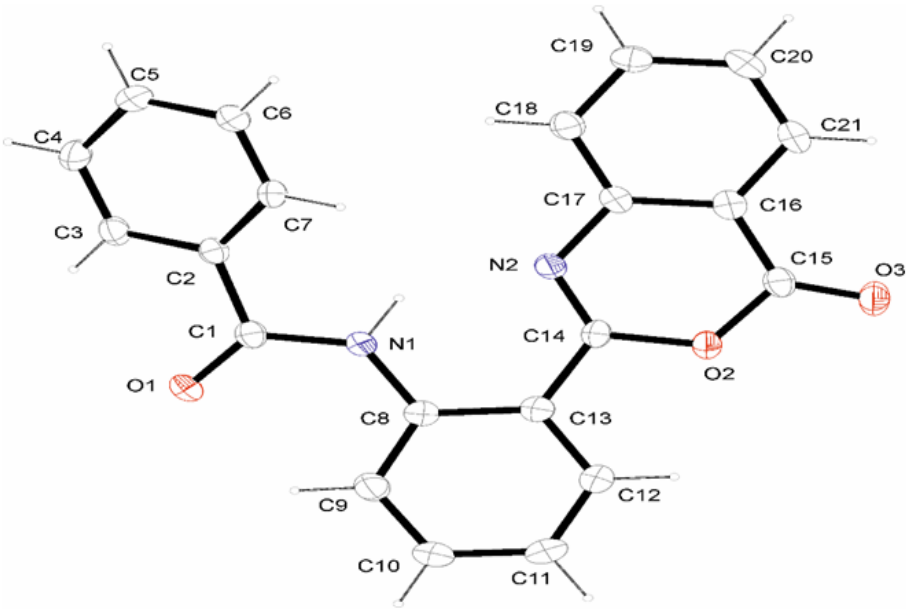

Fig. 4: ORTEP diagram showing the"Butterfly like" conformation of 6a molecule and the numbering scheme.

Docking studies

The ability to successfully handle the intrinsic molecular flexibility of a system and to correctly describe the energetics of receptor-ligand interactions is critical to prospective drug design studies. [25]

The crystal structure of HIV-1 RT in complex with RNA/DNA and nevirapine was obtained from protein data bank (PDB Id: 4PUO), validated for docking (rmsd= 0.21 Å), and used for the docking studies. Docking analysis was carried out using MOE software, version 2019.0101 where the pose with the lowest binding energy was selected as the final docked conformation. Table S1 shows two-dimensional (2D) presentations of the binding between the ligands and the hydrophobic and non- hydrophobic amino acids within NNIBP outlined by Namasvayamet al.[26] The ligands (5a-n) and (6a-n) show ΔG binding scores, in the range -7.67 to -9.35 Kcal/mol, values that are either equal to or higher than the reference nevirapine. Docked nevirapine interacts with the allosteric NNIBP of HIV-1 RT *via* H-π bonding between the dipyridodiazepinone rings and amidic backbone residues of Val106 and Leu234; meanwhile, van der Waals forces influence the binding between its methyl group and Tyr188. On the one hand, the torsion flexibility allowable by five rotatable bonds led to the exposure of the three building blocks in the molecular structures of (5a-n) to bind with the receptor residues of hydrophobic, and/or aromatic nature. On the other hand, in compounds (6a-n) having three rotatable bonds, the right branch R-CONH did not bind to any of the residues, meanwhile, the benzoxazinone and the central phenylene nucleus predominate in the binding process to the same residues bound with (5a-n). The only exception to this was that 6l was found to bind to Lys101 *via* strong hydrogen bonding (Lys-NH_2---O=C(R)NH- ligand of the right branch) and to Lys172 *via* halogen bonding (Lys-NH_2---Cl-ligand of the right branch).

It is worth noting that the molecular docking results of series 5 and 6 show that they do not bind to many of the most frequently mutated amino acids in the allosteric pocket such as Lys103, Tyr181, Gly190, Pro225, Phe227, Met230, and Lys238. However, most of the ligands in these two series of compounds were shown to bind to one or more minor mutants Leu100 and Lys101and the major mutants Val106 and Tyr188,[27] as shown in Table S3.

Molecular orbital and reactivity descriptors

The highest occupied molecular orbital (HOMO), and lowest unoccupied molecular orbital (LUMO) energies play an important role in predicting the chemical and biochemical reactivity of compounds. The optimized molecular geometry of the ligands was characterized at the minimum in energy (minimum RMS gradient 0.100). HOMO and LUMO energy were calculated using Mopac, Chem3D ultra 8.0. The computed HOMO and LUMO energies and other energy descriptors such as ionization potential (I), electron affinity (A), electronegativity (χ), chemical hardness (η), softness (s), chemical potential (μ) and electrophilicity index (ω) were calculated on the basis of the HOMO and LUMO orbital's[28-30] with the results shown in Table S4.

The lowest and highest energy of the developed descriptors of (5a-n) and (6a-n) are summarised in Table 1. The lower energy gap, chemical hardness, and higher softness of series 6 relative to 5 indicate the expected higher reactivity of the benzoxazinones to bind with the NNIBP residues. In effect, from Table S 3 it can be observed that nine compounds 6 d-j, l, and m out of a total 14, exhibit IC_{50} values (half maximal inhibitory concentration) lower than their noncyclized acid precursors 5d-j, l, and m, while two compounds 6k and 5k showed the same IC_{50} values. The higher electron affinity, electronegativity, and electrophilicity indexes [31] of the docked molecules in series 6 correlate with the ability of 11 ligands 6a, d, e - j, l-n to bind with the nucleophilic side chain of the mutant residues Lys101 and Tyr188 in the pocket versus the 6 ligands 5c, e, h, l-n of lower indexes as observed from Table S3**.**

Table 1: Lowest and highest energy descriptors of 5a-n and 6a-n.

Molecular Descriptor	5 a-n	6 a-n
	Lowest / Highest (eV)	Lowest / Highest (eV)
HOMO	−8.512 −9.177	−8.679 −9.148
LUMO	−0.478 −0.608	−1.081 −1.187
ΔE (HOMO_LUMO) (energy gap)	−8.033 −8.569	−7.526 −7.982
I (Ionization potential) = − E_{HOMO}	8.512 9.177	8.679 9.148
A (Electron affinity) = − E_{LUMO}	0.478 0.608	1.081 1.187
χ (Electonegativity) = (I+A)/2	4.495 4.892	4.916 5.160
η (Chemical hardness) = (I− A)/2	4.017 4.285	3.763 3.991
S (Softness)= 1/2 η	0.117 0.124	0.125 0.133
μ (Chemical potential) = − (I+A)/2	−4.495 −4.892	−4.916 −5.160
ω (Electrophilicity) = μ^2 /2 η	2.515 2.793	3.170 3.340

Biological activity

The synthesized compounds 5a–n and 6a–n were evaluated for their WT HIV-1 RT inhibitory activity, with the results shown in Table S3. The 13 compounds 5a, 5c, 5k, 5l, 5n, 6d, 6f, 6g, 6h, and 6j–m exhibit IC_{50} values within the submicromolar range of 0.03–0.72 μM, and the compounds 5b, 5d, 5g, 5h, 5i, 5j, 5m, and 6a–c, 6e, 6i, and 6n show moderate activity, with IC_{50} values in the range of 1.2–7.8 μM, compared with the reference drug nevirapine (IC_{50} = 0.11 μM). The most active compounds, 6d and 6l exhibit IC_{50} values of 30 and 80 nM, respectively, whereas the least active compounds, 5e, and 5f, show IC_{50} values of 123.5 and 17.7 μM, respectively. As shown in Table S1, the binding energy score, ΔG, and the number of bonds between the ligands and residues in the NNIBP do not correlate to the estimated IC_{50} values. This random binding to residues indicates that the activity of the compounds is related to their structural features.[32] In effect, 5a, 5c, 5d, and 5k, wherein the right branch the R moiety features phenyl and electron-donating groups (phenyl for 5a, p-tolyl for 5c, 4-methoxybenzyl for 5d, and 3,4,5-trimethoxyphenyl for 5k), lead to IC_{50} values of 0.37, 0.37, 1.35, and 0.41 μM, respectively. On the other hand, R with electron-withdrawing character (4-chlorophenyl for 5b, 2,4-dichlorobenzyl for 5g, and chloromethyl for 5m) exhibited higher IC_{50} values of 1.37, 4.76, and 3.07 μM, respectively. The decreased RTI activity of the compounds 5b, 5g, and 5m could be related, among other factors, to the reduced interaction between the ligands and residues elicited by the less favorable distribution of electrons. In support of this argument, evident reduction in the enzyme inhibition potential of 5e (R= 2-phenethyl) and 5f (R= 1-naphthylmethyl) was observed, with IC_{50} values of 123.52 and 17.7 μM respectively. In this case, the two and one methylene spacers might disturb the extended conjugation between the bulk of the molecule and the phenyl and naphthyl moieties. However, in series 5 compounds with alkamido R groups (n-pentyl for 5h, n-butyl for 5j, CH_2Cl for 5m, and CH_3 for 5n) showed decreased IC_{50} values in parallel with their decreased chain length opposite to their cLogP values shown in Table 2. This consequence can be attributed to the configurational entropic penalty of the ligands in complex with the binding pocket amino acids since the free energy change on binding is related to both entropic and enthalpic contributions.[33] Theoretical calculations and experimental results pointed out that the penalty of binding entropies of ligand-receptor interactions may correlate with the number of rotatable bonds of chainlike molecules. This correlation depends on the nature of the series of compounds.[34,35] On the contrary to the RTI activity of 5h, 5j, 5m, 5n, the cyclized molecules 6h, 6j, 6m, and 6n, show decreased IC50 values in parallel with the chain length, and the fairly strong linear relationship between cLogP values, and inhibition activity is predicted using Equation (1):

$$\text{Log1/IC}_{50} = -1.900 + 0.477\text{clogP} \quad (1)$$
$$n = 4,\ R = 0.818,\ SE = 0.320$$

where n represents the number of observations, R is the regression correlation coefficient, and SE is the standard error, which indicates that 66.9% of inhibition activity depends on lipophilicity of the molecules. The impact of the bioisosteric replacement of R group 3-pyridyl for phenyl was found to not be in complete agreement with what was expected. The results in Table 2 show the increased IC_{50} of the pyridyl-containing compound 5i versus the variable degrees of improved logS parameter relative to 5a, 5b, and 5c the compounds featuring phenyl and substituted phenyl groups. Of interest, the earlier discussed correlation between the IC50 values and the electronic effect of the R groups in series 5 compounds is not observed for their benzoxazinone analogs 6a–d, 6g, 6k, and 6m. Furthermore, bioisosteric replacement of the 3-pyridyl ring in 6i for phenyl and substituted phenyl groups, as in 6a, 6b, and 6c was accompanied by decreased IC_{50} and improved logS values.

Table 2: HIV-1 RT IC_{50}, physicochemical characters and binding energy score of our ligands with residues within NNIBP.

Compound	IC_{50}(µM)	ΔG score (Kcal/mole)	LogS	cLogP	M.Wt. (g/mol)	Lipinski-Druglikeness	Lipinski-Violation
5a	0.37	-8.57	-5.38	4.1	360.37	1	0
5b	1.37	-8.59	-6.06	4.81	394.81	1	0
5c	0.37	-8.63	-5.72	4.6	374.4	1	0
5d	1.35	-8.95	-5.51	4.06	404.42	1	0
5e	123.52	-9.03	-5.72	4.34	388.42	1	0
5f	17.73	-8.74	-6.75	5.24	424.46	1	1
5g	4.76	-8.17	-6.8	5.55	443.29	1	1
5h	5.1	-8.06	-4.98	4.3	354.41	1	0
5i	2.01	-8.47	-5.06	3.41	361.36	1	0
5j	7.86	-8.52	-4.65	3.78	340.38	1	0
5k	0.41	-9.35	-5.68	3.96	450.45	1	0
5l	0.24	-8.23	-9.32	7.32	596.04	0	2
5m	3.07	-8.23	-4.3	3.11	332.74	1	0
5n	0.57	-7.67	-3.74	2.5	298.3	1	0
6a	2.37	-8.43	-6.18	5.02	342.35	1	0
6b	3.4	-8.63	-6.86	5.73	376.8	1	1
6c	2.38	-8.69	-6.52	5.52	356.38	1	1
6d	0.03	-8.74	-6.31	4.98	386.41	1	0
6e	1.24	-8.63	-6.52	5.25	370.41	1	1
6f	0.66	-8.33	-7.55	6.16	406.44	1	1
6g	0.72	-8.35	-7.6	6.47	425.27	1	1
6h	0.36	-8.34	-5.78	5.21	336.39	1	1
6i	1.21	-8.54	-5.86	4.33	343.34	1	0
6j	0.43	-8.3	-5.45	4.7	322.36	1	0
6k	0.44	-8.89	-6.48	4.88	432.43	1	0
6l	0.08	-8.19	-10.11	8.24	578.02	0	2
6m	0.42	-7.67	-5.09	4.03	314.73	1	0
6n	3.24	-7.67	-4.53	3.42	280.28	1	0

The measured druggability values of the prepared compounds 5a–n and 6a–n shown in Table 2 indicate that all of the prepared compounds meet the requirements of the Lipinski drug-likeness structural features,[36,37] with the exception of compounds 5l and 6l, which showed molecular weight and cLogP beyond limits. The potential cytotoxicity values, CC_{50} (concentration that reduced the cell viability by 50%), of the selected active and druggable ligands 5a, 6d, 6h, and 6k were determined using colorimetric viability assay after their incubation with HeLa cells for a period of 24 hrs. Figure 5 shows the inhibition dose-response curves of the most active inhibitors *versus* the HeLa cell viability. Low cytotoxicity of the compounds is demonstrated by the high SI (selectivity index) (CC_{50} / IC_{50}), as shown in Table 3.

Table 3: CC_{50} of the selected druggble active ligands.

Compd. No	**Druggability**	**IC_{50} (µM)**	**CC_{50} (µM)**	**SI = (CC_{50}/ IC_{50})**
5a[a]	1	0.37	518.1	1400
6d	1	0.03	970	32333
6h	1	0.36	298.2	828
6k	1	0.44	261.8	595

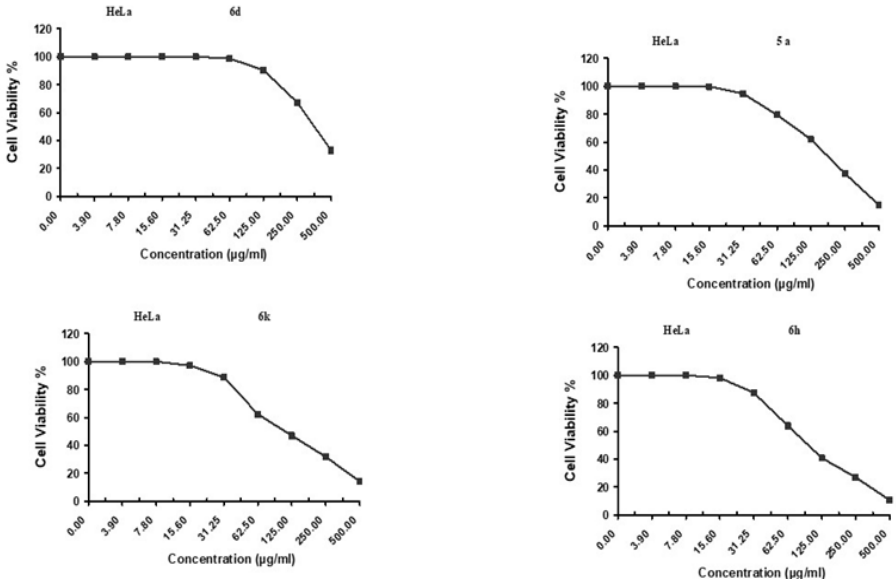

Fig. 5: Inhibition dose respons curves versus HeLa cell viability of 5a, 6d, 6h and 6k.

The relationship between the molecular structure and activity can be highlighted by the following observations:

1- The compounds with aryl R groups in series 5 are active with submicromolar IC_{50} values, whereas series 6 compounds that exhibit submicromolar IC_{50} values featured aralkyl and heteroaryl R groups. Table 4 summarizes the impact of the R group on the IC_{50} value.

2- The methoxyaryl fragment yielded the active molecules 5d , 5k, 5l, , 6d, 6k, and 6l having IC_{50} 1.35, 0.41, 0.24, 0.03, 0.44, and 0.08 µM respectively. Methoxy-indolyl moiety in 5l and 6l led to distinctly reduced IC_{50}.

3- Bioisosteric replacement of 3-pyridinyl nucleus in 5i and 6i for phenyl and the substituted phenyl nuclei, affects RTI activity. The IC_{50} value of 5i is 1.4 -5.4 times of the phenyl derivatives 5a, 5b, and 5c whereas the IC_{50} of 6i is 0.36-0.51 times that of the phenyl analogs 6a, 6b, 6c. The presence of the pyridine nucleus led to improved solubility LogS values of the compounds in both series

4- . The increased number of benzoxazinone molecules 6 with low IC_{50} values can be predicted by their decreased energy gap ΔE, decreased hardness, and increased softness indicating enhanced noncovalent bonding with the NNIBP residues relative to molecules of series 5 compounds.

5- As an outcome of the docking study, the number of molecules that contribute to the binding of the nucleophilic side chains of Lys101 and Tyr188 is in good agreement with the higher electron affinity, electro-negativity, and global electrophilicity of molecules of series 6 compounds compared with those of series5.

Table 4: Impact of R on the IC_{50} of the ligands **5a-n** and **6a-n**.

Nature of R	5a-n		6a-n	
	R	[a] IC_{50} (µM)	R	[a] IC_{50} (µM)
nAlkyl	Me << $ClCH_2$<Pentyl <Butyl	0.57; 3.07; 5.10; 7.86	Pentyl < $ClCH_2$ < Butyl << Me	0.36; 0.42; 0.43; 3.25
Aryl	Ph, *p*-Tolyl < 3,4,5-$(OMe)_3$Ph <*p*-ClPh	0.37; 0.37; 0.41; 1.37	3,4,5-$(OMe)_3$Ph << Ph, *p*-Tolyl << *p*-ClPh	0.44; 2.37; 2.38; 3.40
Heteroaryl	Substituted indolyl <<3-pyridinyl	0.24; 2.01	Substituted Indolyl << 3-pyridinyl	0.08, 1.21
Aralkyl	*p*-MeOBn < 2,4-ClBn <<< Nphthyl-1-CH_2 << $PhCH_2$-CH_2	1.35; 4.76; 17.73; 123.5	*p*-MeOBn << Nphthyl-1-CH_2 < 2,4-ClBn < $PhCH_2$-CH_2	0.03; 0.66; 0.72; 1.24

[a] arranged in the same order displayed by R

Conclusion

In the present study, we synthesized 28 compounds of two new subclasses of NNRTIs. N-acylation of the key compound anthranoylanthranilic acid yielded the chainlike diamide N-acylanthranoylanthranilic acid series of the compounds **5a-n**. By cyclodehydration of the members of the first series, we obtained the bezoxazin-4-one **6a-n** compounds. The assigned structure for the benzoxazin-4-ones was unequivocally confirmed by HMBC spectrum and X-ray crystallography. Docked molecules have avoided binding to most of the recognized mutant amino acids in W HIV-1 RT. However, binding to one or more of the minor Leu100 and Lys101 and the major Val106 and Tyr188 mutants was not completely evaded. The values of NNRTI activity index IC_{50} within each of the two series of compounds were affected by a different extent ensued from the nature of the N-acyl moieties. The IC_{50} of benzoxazinone ligands in series **6** was enhanced by the moieties aralkyl (IC_{50}= 0.030 -1.24 µM), and heteroaryl (IC_{50}= 0.08-1.21 µM), while in the case of the anthranoylanthranilic acid ligands in series **5,** the aryl moiety yielded the most active molecules (IC_{50}= 0.37-1.37 µM).

Molecular orbital calculations indicated higher reactivity of the majority of molecules in series **6** relative to series **5**. Interaction of ligands with nucleophilic side chains of the most frequently mutated residues Lys 101 and Tyr188 in the NNIBP was predicted by the calculated electron affinity, electronegativity, and electrophilicity energy derived parameters of ligands. These features seem of value in insilico studies and further development of mutation-resistant leads.

Very low cytotoxicity of the most active and druggable compounds **5a**, **6d**, **6h**, and **6k** was characterized by the high selectivity index SI. The submicromolar active compounds having low toxicity, short and simple synthesis, and consumed commercially available chemicals uncover promising hits for developing new effective HIV-1 NNRTI.

Acknowledgment

We would like to express our gratitude and appreciation to Dr. Ahmed Safwat, Medicinal Chemistry, Faculty of Pharmacy, Assiut University, for mentoring molecular modeling. The authors are very grateful to Alexander von Humboldt Foundation for supporting Georg Forster Research Fellowship for the experienced researcher.

Conflict of interest

There are no conflicts to declare.

Note: Table numbers preceded by the letter S are looked for as Supplementary material and are available on request from the corresponding author.

REFERENCES

1. The Global HIV/AIDS Epidemic,HIV.gov. updated, July 7 (2020).
2. *a)* C. Beyrer and A. Pozniak, "HIV drug resistance—an emerging threat to epidemic control", ***N Engl J Med,*** 377,1605-1607 (2017). DOI: 10.1056/NEJMp1710608; *b)* C. Wymant, D. Bezemer , F. Blanquart *et al*., ***Science*** 375, 540–545 (2022). Doi: 10.1126/science.abk1688.
3. *a)* Global HIV/AIDS Overview | HIV.gov; *b)* J.G. Hoogeveen, and L.-A.Gladys eds, "Distributional Impacts of COVID-19 in the Middle East and North Africa Region". MENA Development Report. Washington, DC: World Bank. Doi:10.1596/978-1-4648-1776-2.
4. T. Ndung'u, J. M. McCune, and S.G. Deeks, "Why and where an HIV cure is needed and how it might be achieved". ***Nature,*** 576(7787), 397-405 (2019). DOI: 10.1038/s41586-019-1841-8
5. FDA - Approved HIV Medicines / NIH, https://hivinfo.nih.gov/understanding-hiv/fact-sheets/fda-approved-hiv-medicines, Last reviewed Agust 24 (2021).
6. F. Esposito, A. Corona, and E. Tramontano, "HIV-1 reverse transcriptase still remains a new drug target: structure, function, classical inhibitors, and new inhibitors with innovative mechanisms of actions", ***Mol Biol Int***, 2012, 586401 (2012).
7. D. Kang, D. Feng, T. Ginex, J. Zou, F. Wei, T. Zhao, *et al*., "Exploring the hydrophobic channel of NNIBP leads to the discovery of novel piperidine-substituted thiophene [3, 2-d] pyrimidine

derivatives as potent HIV-1 NNRTIs", ***Acta Pharm Sin B,*** 10(5)**,** 878-894 (2020). DOI: 10.1016/j.apsb.2019.08.013

8. P. Gerondelis, R.H. Archer, C. Palaniappan, *et al.*, "The P236L delavirdine-resistant human immunodeficiency virus type 1 mutant is replication defective and demonstrates alterations in both RNA 5′-end-and DNA 3′-end-directed RNase H activities", ***J Virol,*** 73(7)**,** 5803-5813 (1999).
9. P. Shirvani, A. Fassihi, and L. Saghaie, "Recent Advances in the Design and Development of Non-nucleoside Reverse Transcriptase Inhibitor Scaffolds", ***Chem Med Chem,*** 14(1), 52-77 (2019). Doi: 10.1002/cmdc.201800577.
10. B. Qin, X. Jiang, H. Lu, et al., "Diarylaniline derivatives as a distinct class of HIV-1 non-nucleoside reverse transcriptase inhibitors", ***J Med Chem***, 53(13), 4906-4916 (2010). DOI: 10.1021/jm1002952.
11. C. Zhuang, C. Pannecouque, E. De Clercq and F. Chen, "Development of non-nucleoside reverse transcriptase inhibitors (NNRTIs): our past twenty years", ***Acta Pharm.Sin B,*** 10(6), 961-978 (2020). DOI: 10.1016/j.apsb.2019.11.010.
12. D. Kang, D. Feng, Y. Sun, *et al*., "Structure-based bioisosterism yields HIV-1 NNRTIs with improved drug-resistance profiles and favorable pharmacokinetic properties", ***J Med Chem,*** 63(9)**,** 4837-4848 (2020). DOI: 10.1021/acs.jmedchem.0c00117.
13. C.T. Öberg, M. Strand, E.K. Andersson, *et al*., "Synthesis, biological evaluation, and structure–activity relationships of 2-[2-(benzoylamino) benzoylamino] benzoic acid analogues as inhibitors of adenovirus replication", ***J Med Chem,*** 55(7), 3170-3181 (2012). Doi.org/10.1021/jm201636v.
14. S. Zuffanti, "Preparation of acyl chlorides with thionyl chloride", ***J Chem Educ,*** 25(9)**,**481(1948). Doi.org/10.1021/ed025p481.
15. G.M.Coppola, "The chemistry of 4H-3, 1-benzoxazin-4-ones". J**.** ***Heterocycl. Chem.,*** 36(3), 563-588 (1999). https://doi.org/10.1002/jhet.5570360301.
16. Meyer, Graf , Biochemische Zeitschrift, 154-156 (1930).
17. A. A.-M. Abdel-Hafez, "An efficient, convenient synthesis of novel medium-sized13H-dibenzo[d,h][1,3,7] oxadiazecine-8, 14-dione macrolides as anticipated antineoplastic agents", ***Bioorg Med Chem,*** 10(7)**,** 2297-2302 (2002).
18. M.A. El-Hashash and D.B. Guirguis, "Synthesis And Reactions of 2-(4-Bromophenyl)-4H-3, 1-Benzoxazine-4-one*″*, ***Eur. Chem. Bull.,*** 2(9)**,** 651-656 (2013).
19. M.N. Khimich, E.A. Birgen, B.M. Bolotin, and B.M. Uzhinov, "Intramolecular photoinduced proton transfer in 2-(2-aminophenyl)-4H-3, 1-benzoxazin-4-ones with different electron-withdrawing N-substituents*″*, ***High Energy Chem,*** 43(2), 123-128 (2009).
20**.** Roche, "Reverse Transcriptase Assay, Colorimetric enzyme immunoassay for the quantitative determination of retroviral reverse transcriptase activity by incorporation of digoxigenin- and biotin-labeled dUTP into DNA sigma-aldrich.com"; Version 14, 14-15, (May 2016).
21. T. Mosmann, "Rapid colorimetric assay for cellular growth and survival: application proliferation and cytotoxicity assays", ***J Immunol Methods,*** 65(1-2)**,** 55-63 (1983). DOI: 10.1016/0022-1759(83)90303-4.
22. R.P. Staiger and E.B. Miller, "Isatoic anhydride. IV. Reactions with various nucleophiles", ***J OC,*** 24(9)**,** 1214-1219 (1959). Doi.org/10.1021/jo01091a013.
23. J.K. Annor-Gyamfi, and R.A. Bunce, "4H-Benzo [d][1, 3] oxazin-4-ones and Dihydro Analogs from Substituted Anthranilic Acids and Orthoesters", ***Molecules,*** 24(19)**,** 3555 (2019). Doi.org/10.3390/molecules24193555.
24. J. Balzarini, B. Orzeszko-Krzesińska, J.K. Maurin and A.Orzeszk, "Synthesis and anti-HIV studies of 2- and 3-adamantyl-substituted thiazolidin-4-ones", ***Eur J Med Chem,*** 44(1), 303-311(2009). Doi:10.1016/j.ejmech.2008.02.039.
25. A.N.Jain and A.Nicholls, "Recommendations for evaluation of computational methods. J. Comput", ***Aided Mol Des,*** 22(3-4), 133-139 (2008). DOI 10.1007/s10822-008-9196-5.

26. V. Namasivayam, M. Vanangamudi, V.G. Kramer, *et al*. "The journey of HIV-1 non-nucleoside reverse transcriptase inhibitors (NNRTIs) from lab to clinic", ***J Med Chem,*** 62(10)**,** 4851-4883 (2019). Doi:10.1021/acs.jmedchem.8b00843.
27. L. Battini and M. Bollini, "Challenges and approaches in the discovery of human immunodeficiency virus type-1 non-nucleoside reverse transcriptase inhibitors", ***Med Res Rev.,***39(4),1235-1273 (2019). DOI: 10.1002/med.21544.
28. M. Miar, A. Shiroudi, K. Pourshamsian *et al.*, "Theoretical investigations on the HOMO–LUMO gap and global reactivity descriptor studies, natural bond orbital, and nucleus-independent chemical shifts analyses of 3-phenylbenzo [d] thiazole-2 (3H)-imine and its para-substituted derivatives: Solvent and substituent effects", ***J Cem Res,*** 147-158 (2021). DOI:10.1177/1747519820932091.
29. P.K. Chattaraj, S. Giri, and S. Duley, "Update 2 of: electrophilicity index", ***Chem Rev,*** 111(2), Pr43-Pr75 (2011).
30. R. Świsłocka, E. Regulska, J. Karpińska, G.Świderski,and W. Lewandowski, "Molecular structure and antioxidant properties of alkali metal salts of rosmarinic acid. Experimental and DFT studies", ***Molecules,*** 24(14)**,** 2645 (2019).
31- R.G. Parr , L.V. Szentpály, and S. Liu, "Electrophilicity index", ***J Am Chem Soc,*** 121**,** 1922-1924 (1999).
32. *a)* A.Paneth, W. Płonka, and P. Paneth, "Assessment of nonnucleoside inhibitors binding to HIV-1 reverse transcriptase using HYDE scoring", ***Pharmaceuticals,*** 12(2)**,** 64 (2019). *b)* C. Gao, M.-S. Park, and H.A. Stern, "Accounting for ligand conformational restriction in calculations of protein-ligand binding affinities", ***Biophys J,*** 98(5), 901-910 (2010).
33. *a)*D. L. Mobley, and K. A. Dill, "Binding of Small-Molecule Ligands to Proteins: "What You See"Is Not Always "What You Get"", ***Structure***, 17(4), 489–498 (2009). Doi:10.1016/j.str.2009.02.010. *b)* D. H. Williams, E. Stephens, D. P. O_Brien, and M. Zhou, "Understanding Noncovalent Interactions: Ligand Binding Energy and Catalytic Efficiency from Ligand-Induced Reductions in Motion within Receptors and Enzymes", ***Angew Chem Int Ed,*** 43(48),6596–6616(2004).DOI: 10.1002/anie.200300644.
34. C.-en A. Chang, W. Chen, and M.K. Gilson, "Ligand configurational entropy and protein binding", ***PNAS,*** 104(5), 1534–1539(2007). Doi.org/10.1073/pnas.0610494104
35. C.-En Chang, and M.K. Gilson, "Free Energy, Entropy, and Induced Fit in Host-Guest Recognition: Calculations with the Second-Generation Mining Minima Algorithm", ***J Am Chem Soc,*** 126(40), 13156-13164(2004). https://doi.org/10.1021/ja047115d.
36. C.A. Lipinski, F. Lombardo, B.W. Dominy and P. J. Feeney, "Experimental and computational approaches to estimate solubility and permeability in drug discovery and development settings", ***Ad. Drug Deliv Rev,*** 46(1-3), 3-26 (1997).
37. C.A. Lipinski, "Lead-and drug-like compounds: the rule-of-five revolution", ***Drug Discov Today Technol,*** 1(4)**,** 337-341(2004).Doi: 10.1016/j.ddtec.2004.11.007.

Bull. Pharm. Sci., Assiut University, Vol. 45, Issue 1, 2022, pp. 201-222.

نشرة العلوم الصيدلية
جامعة أسيوط

BULL. PHARM. SCI. Assiut Univ.

تشييد، دراسة النمذجة الجزيئية، والتقييم البيولوجي لمشتقات حمض ن-أسيل أنثرا نويل أنثرا نيليك و نواتج تحولها الى بنزوكسازينونات كمثبطات جديدة لانزيم الترانسكريبتيز المنعكس الغير نيوكلوزيدي

حسام محمد حسن عبد العزيز[1،2]- احمد مجدي أحمد محمد[1]- عاطف عبد المنعم عبد الحافظ[1]- عادل فوزي يوسف[1]

[1]قسم الكيمياء الدوائية ، كلية الصيدلة ، جامعة أسيوط، مصر

[2]قسم الكيمياء الطبية، كلية الصيدلة ، جامعة قنا ، مصر

بالرغم من كفاءة مضادات الفيروسات المستعملة في منع انتشار فيروس نقص المناعة المكتسبة الادمي الا انه لا يوجد علاج فاعل من الإصابة حتى الان. أخذين في الاعتبار هذا الواقع فقد تم تشييد ٢٨ مركبا من مشتقات حمض ن-أسيل أنثرا نويل أنثرا نيليك و نواتج تحلقه: ال- بنزوكسازينونات و تم تقييمها كعوامل كبت انزيم الترانسكريبتيز المنعكس الغير نيوكلوزيدي (IC_{50}) كما تم تقييم معامل السمية (CC_{50}) للمركبات الأكثر فعالية والتي توافق خواصها مع قاعدة ليبنسكي. كما أمكن تبرير الفعالية الأكثر التي ظهرت بين مجموعة ال بنزوكسازينونات كمثبطات للإنزيم وكذلك قابلية الارتباط مع بقايا محبات النواه في الموقع الخفي المجاور للموقع النشط لإنزيم الترانسكريبتيز المنعكس.

ملاحظة: الجداول التكميلية والمسبوق أرقمها بالحرف S ممكن طلبها من الباحث المقابل.